Lithos 338–339 (2019) 73–86

Contents lists available at ScienceDirect

Lithos

journal homepage: www.elsevier.com/locate/lithos

Mixed and recycled detrital zircons in the Paleozoic rocks of the Eastern Moroccan Meseta: Paleogeographic inferences

Cristina Accotto [a,*], David Jesús Martínez Poyatos [a], Antonio Azor [a], Cristina Talavera [b,c], Noreen Joyce Evans [c,d], Antonio Jabaloy-Sánchez [a], Ali Azdimousa [e], Abdelfatah Tahiri [f], Hassan El Hadi [g]

[a] Department of Geodynamics, University of Granada, Granada, Spain
[b] School of Geosciences, University of Edinburgh, Edinburgh, UK
[c] John de Laeter Centre, Curtin University, Bentley, Australia
[d] School of Earth and Planetary Science, John the Laeter Centre, Curtin University, Perth, Australia
[e] Faculté Pluridisciplinaire de Nador et Laboratoire des Géosciences Appliquées, Faculté des Sciences, Université Mohammed I, Oujda, Morocco
[f] Geo-Biodiversity and Natural Patrimony Laboratory (GeoBio), Scientific Institute, Geophysics, Natural Patrimony Research Center (GEOPAC) Mohammed V University, Rabat, Morocco
[g] Faculté des Sciences Ben M'Sik, Université Hassan II, Casablanca, Morocco

ARTICLE INFO

Article history:
Received 22 January 2019
Accepted 10 April 2019
Available online 16 April 2019

Keywords:
Eastern Moroccan Meseta
Paleozoic paleogeography
West African Craton
U-Pb geochronology
Zircon provenance

ABSTRACT

The paleogeographic evolution of the Moroccan Variscides has been a matter of discussion for several decades, with current theories mostly based on classical geological correlations. In this regard, the scarce number of studies devoted to U-Pb geochronological analyses of detrital zircon populations is particularly limiting when trying to ascribe the different domains to a single continental piece either derived from the West African Craton or to different sources, with some located in the Nubian Shield or the Saharan Metacraton. In this work, detrital zircon grains from 10 samples of sandstones from the Paleozoic (Ordovician to Devonian) sequence of the Eastern Meseta and Middle Atlas were dated in order to identify possible sediment sources and elucidate the paleogeography of this easternmost portion of the Moroccan Variscides. The main detrital zircon populations have Ediacaran-Cryogenian ages (610–670 Ma, related to the Cadomian and/or Pan-African orogeny) and middle Paleoproterozoic ages (1980–2080 Ma, related to the Eburnean orogeny), which are in agreement with previous data from the Western Meseta, suggesting similarity between both Mesetas, and strong West African Craton affinity. Such an affinity verifies the most accepted paleogeographic interpretation considering that the Moroccan Mesetas remained attached to northern Gondwana during the entire Paleozoic period. The main differences between our samples and those from the Western Meseta concern the minor detrital zircon populations, such as the Cambro-Ordovician and the Tonian-Stenian ones. In particular, Eastern Meseta and Middle Atlas samples lack a Cambro-Ordovician detrital zircon population, usually interpreted as related to the rifting that opened the Rheic Ocean. This population is locally reported in the Western Meseta and widely described in southwestern Europe, where magmatism of this age is well known. Furthermore, the most northeastern samples are also characterized by a Tonian-Stenian detrital zircon population (up to 30% of the data), which might imply northeastern African sources (Saharan Metacraton and/or Arabian-Nubian Shield).

1. Introduction

Zircon is a very common accessory mineral, formed in a wide range of magmatic and metamorphic rocks in orogenic crustal growth areas, and very commonly present in sedimentary detrital rocks, which combined with its strong physical and chemical endurance, make it a valuable tool for geochronological and paleogeographic studies (*e.g.* Avigad et al., 2003; Fernández-Suárez et al., 2002; Linnemann et al., 2004). Detrital zircon grains in sedimentary rocks might have survived a number of sedimentary cycles, preserving primary source signatures. In addition, technological improvements in analytical methods (*e.g.* LA-ICPMS, SHRIMP) have permitted a wide application of detrital zircon geochronology in paleogeographic and geodynamic reconstructions (*e.g.* Fedo et al., 2003), carried out by comparing statistically meaningful detrital zircon age populations with those of possible source areas. This technique has been widely applied to Variscan terranes in central and southern Europe (*e.g.* Braid et al., 2011; Fernández-Suárez et al., 2014; Linnemann et al., 2004, 2008; Pereira et al., 2017; Pérez-Cáceres et al., 2017; Shaw et al., 2014), but only a few works have focused on the Moroccan Meseta Variscides (ensemble of the Variscan domains cropping

* Corresponding author.
E-mail address: accotto@ugr.es (C. Accotto).

https://doi.org/10.1016/j.lithos.2019.04.011
0024-4937/

out in Morocco; *e.g.* El Houicha et al., 2018; Ghienne et al., 2018; Letsch et al., 2018; Pérez-Cáceres et al., 2017).

A magmatic arc was active in the northern margin of the Gondwanan continent during Ediacaran times (*i.e.* Cadomian orogeny). Later, a new Wilson cycle began with the fragmentation of Gondwana during the Cambro-Ordovician rifting that preceded the opening of the Rheic Ocean and the drifting of Gondwana-derived terranes (Franke et al., 2017; Matte, 2001; Murphy et al., 2004; Nance et al., 2012). During the Devonian, subduction narrowed the Rheic Ocean, culminating in continental collision during Carboniferous times (Variscan-Alleghanian orogeny). On a broad scale, this collision involved the northern margin of Gondwana and the southern margin of Laurussia (already docked Gondwana-derived terranes, Laurentia and Baltica), leading to the assembly of the Pangea supercontinent (Franke et al., 2017; Matte, 2001; Nance et al., 2012).

The northwestern African Variscides are considered the southern termination of the Variscan Belt (Matte, 2001), and usually divided into six structural domains (Fig. 1A; Hoepffner et al., 2006): (i) the Sehoul Block, or Caledonian block, characterized by a Caledonian tectonothermal imprint (Michard et al., 2010b; Simancas et al., 2005; Tahiri et al., 2010) and juxtaposed with the Moroccan Meseta domains along the Late-Variscan Rabat-Tiflet Fault Zone; (ii) the Coastal Block (considered the western part of the Western Meseta *s.l.*; Michard et al., 2010b), weakly deformed by the Variscan orogeny and limited to the east by the Western Meseta Shear Zone; (iii) the Central zone of the Western Meseta, deformed by fold and thrusts and bounded to the east by the so-called Nappe Zone and the Tazekka-Bsabis-Bekrit Fault Zone (TBBFZ), located in the Middle Atlas (Michard et al., 2010b); (iv) the Eastern Meseta domain, characterized by small and variably deformed Paleozoic outcrops; (v) the Southern Zone (Hoepffner et al., 2006; Michard et al., 2008), bounded to the north by the Atlas Paleozoic Transform Zone (APTZ) and to the south by the South Moroccan Variscan Front (SMF), which separates the Variscan domains from the almost undeformed Anti-Atlas foreland (Fig. 1A); and (vi) the Mauritanides belt (Villeneuve, 2008), located west of the West African Craton (WAC) and extending from southern Morocco to Senegal (not represented in Fig. 1A).

The pre-Variscan paleogeographic evolution of the Moroccan Mesetas was studied by several authors (*e.g.* El Hassani et al., 2003; Hoepffner et al., 2006; Michard, 1976; Michard et al., 1989, 2010a, 2010b; Piqué, 2001; Piqué and Michard, 1981, 1989; Simancas et al., 2005, 2009; Walliser et al., 1995, 2000), who suggested that they were

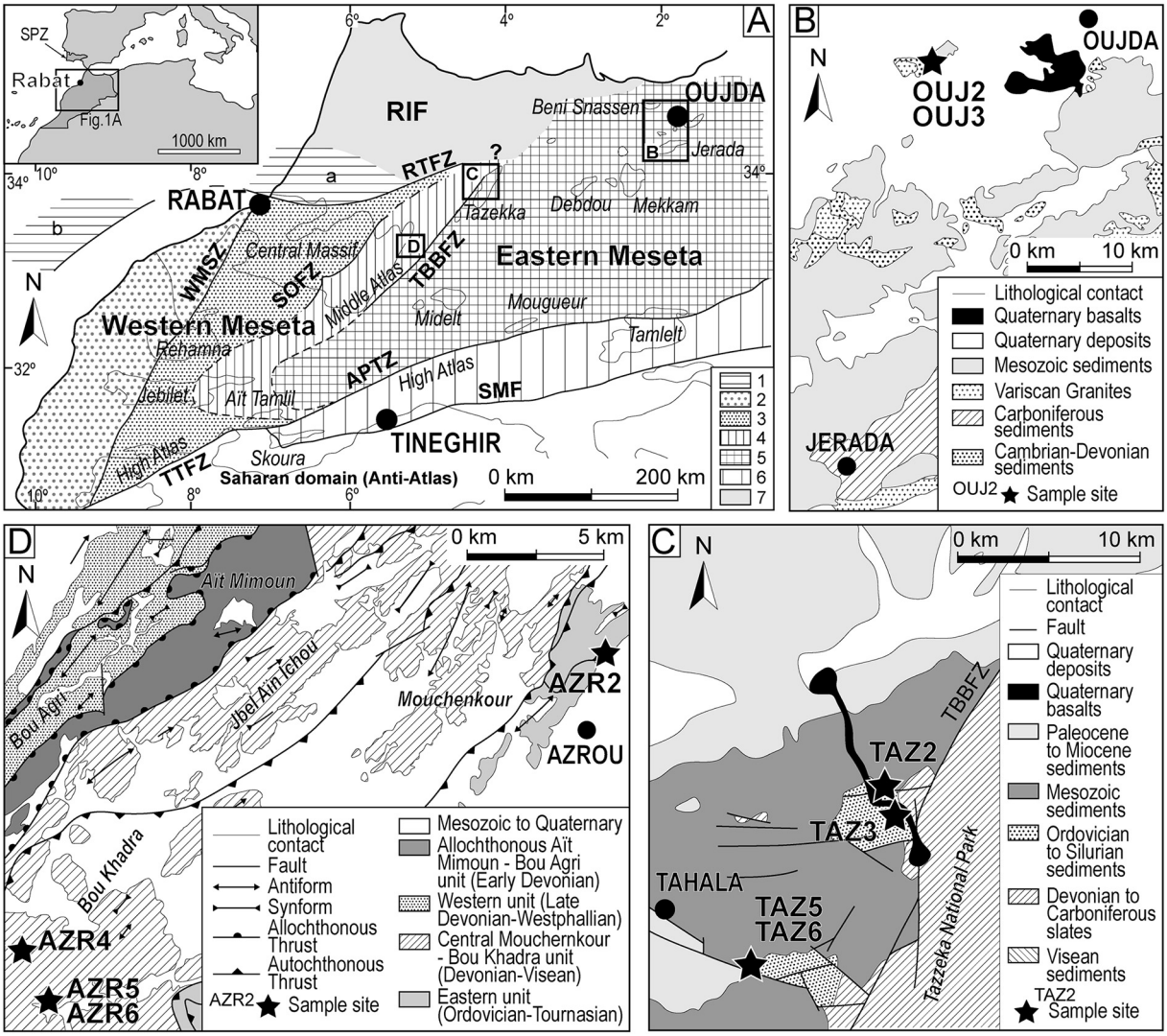

Fig. 1. Geological maps of the northwestern African Variscides with sampling areas. (A) Structural domains (modified from Hoepffner et al., 2006; Michard et al., 2010b). 1: Sehoul Block (a) and Mazagan escarpment (b); 2: Coastal Block; 3: Central zone; 4: Nappe Zone; 5: Eastern Meseta; 6: Southern Zone; 7: Rif Belt. Main structural features: Rabat-Tiflet Fault Zone (RTFZ); Western Meseta Shear Zone (WMSZ); Smaala-Oulmès Fault Zone (SOFZ); Tazekka-Bsabis-Bekrit Fault Zone (TBBFZ); Atlas Paleozoic Transform Zone (APTZ); South Moroccan Front (SMF); Tizin'Test Fault Zone (TTFZ); SPZ: South Portuguese Zone. Black boxes refer to the detailed geological sketches of the sampling areas: (B) Oujda area (after Kharbouch et al., 1989); (C) Tazekka area (after Vidal and Hoepffner, 1979); (D) Azrou area (after Bouabdelli et al., 1989).

part of the northern margin of Gondwana because of the stratigraphic similarity that they share with other autochthonous Gondwanan domains (*e.g.* Anti-Atlas Variscan foreland; Fig. 1A). Further evidence supporting this paleogeographic attribution is the absence of Variscan ophiolitic and/or high-pressure metamorphic rocks indicating the presence of suture zones separating the Moroccan Meseta domains and the foreland (Michard et al., 2010a, 2010b; Simancas et al., 2009). From Cambrian to Devonian times, the entire region was a passive margin (Hoepffner et al., 2005, 2006; Michard et al., 2010b; Piqué, 2001) characterized, from a stratigraphic point of view, by mainly Cambrian-Silurian detrital sequences with some hiatuses, *e.g.* the regression tied to the Late Ordovician glaciation (Le Heron, 2007; Le Heron et al., 2009). The stratigraphic sequences of the Moroccan Meseta domains began to differentiate during the Devonian, which is characterized by reefal platform facies in the Western Meseta, and by more basinal facies in the Eastern Meseta (Hoepffner et al., 2005, 2006; Michard et al., 2010b; Piqué, 2001). From a structural point of view and according to Michard et al. (2010b), the Moroccan Meseta domains were originally separated by narrow Early Paleozoic thinned-crust zones, probably related to incipient intra-continental rifting, which were later reactivated as shear zones during the Variscan orogeny. To the south, the Moroccan Meseta domains were separated from the Anti-Atlas foreland by a major intra-continental fault corresponding to the SMF, a polyphasic crustal-scale flower-structure characterized by dextral transpressive kinematics (Houari and Hoepffner, 2003) with a minimum offset of tens of kilometers (Michard et al., 2010b).

In this context where different domains are recognized, detrital zircon dates become a helpful tool to identify the main source areas of the sediments and, therefore, their paleogeographic affinities. In particular, the WAC affinity is usually characterized by Ediacaran-Cryogenian and Paleoproterozoic peaks, as well as a general Mesoproterozoic gap in the age distribution pattern. However, it must be noticed that detrital zircon populations of this age (1.0–1.5 Ga) were locally described by Bradley et al. (2015) in the Ediacaran clastic sequences unconformably overlying the western part of the WAC basement in Mauritania. The source of these Mesoproterozoic detrital zircons is unlikely the WAC basement, since primary sources of that age are unknown in the WAC, and relevant Mesoproterozoic detrital zircon populations have not been detected in Ediacaran/Paleozoic sediments located to the North of the WAC and derived from it (see below). Therefore, suitable sources for these Mesoproterozoic zircons could be the Amazonian basements adjoining western Gondwana at Ediacaran time.

In the Moroccan Variscides north of the WAC, most of the previous detrital zircon studies focused on Cambro-Ordovician and Precambrian sedimentary sequences from the Anti-Atlas (Abati et al., 2010; Avigad et al., 2012), Middle Atlas, Western Meseta and Coastal Block (El Houicha et al., 2018; Ghienne et al., 2018; Letsch et al., 2018), all of them having highlighted a strong WAC affinity. Very similar results were obtained on Triassic sandstones and siltstones of the High Atlas (Domènech et al., 2018; Marzoli et al., 2017) and Middle Atlas (Pratt et al., 2015). Furthermore, Avigad et al. (2012), Marzoli et al. (2017), and Ghienne et al. (2018) also identified, on Middle Cambrian sandstones and siltstones (Anti-Atlas), Late Triassic siltstones (High Altas), and Late Ordovician sandstones (Middle Atlas) respectively, a minor 1.1–0.9 Ga detrital zircon population that they attributed to distal north-eastern African sources, probably located in the Precambrian basement of the Saharan Metacraton or the Arabian-Nubian Shield (Bea et al., 2010; Linnemann et al., 2011). In the Central zone of the Western Moroccan Meseta (Fig. 1A), an unimodal detrital zircon population centered around 488 Ma was recognized in a Lower Paleozoic greywacke (Letsch et al., 2018), and Late Cambrian granite boulders in a Devonian conglomerate were dated by Tahiri et al. (2017). These pieces of evidence suggest the presence of a nearby and unknown igneous Late Cambrian source. A few Cambro-Ordovician detrital zircon grains were also found in the Middle Atlas in Late Ordovician sandstones of the Tifarouine Formation (Ghienne et al., 2018) and in Middle Jurassic sandstones of the Bou Rached Formation (Pratt et al., 2015). These Cambro-Ordovician ages have been interpreted as evidence of magmatism related to the continental rifting that preceded the opening of the Rheic Ocean (*e.g.* Cambeses et al., 2017; Nance et al., 2010, 2012). Finally, U-Pb zircon ages from Cambrian sandstones of the Sehoul Block (Pérez-Cáceres et al., 2017) also show main Ediacaran and Paleoproterozoic peaks, together with a very minor 1.1–0.9 Ga population and scattered Archean data, suggesting that this terrane was close to the Gondwana margin at Cambrian time.

Despite the new advances, the paleogeographic interpretation of the Moroccan Variscides is still a matter of debate and lacks data, in particular from the Paleozoic sedimentary sequences of the Eastern Meseta. In this paper we present the first U-Pb detrital zircon ages for Ordovician sedimentary rocks from the Eastern Meseta (Oujda area; Figure1B) and new data from the Ordovician to Devonian sequence cropping out at the boundary between the Eastern and Western Mesetas (Middle Atlas: Tazekka and Azrou massifs; Fig. 1C and D).

2. Geological setting

The Moroccan Mesetas (Fig. 1A; Hoepffner et al., 2006) include scarce outcrops of Precambrian basement (mainly igneous Cadomian rocks) unconformably overlain by Cambro-Devonian sedimentary rocks (Chopin et al., 2014; El Houicha et al., 2018; Hoepffner et al., 2005; Letsch et al., 2018; Michard et al., 2008, 2010b; Ouabid et al., 2017; Pereira et al., 2015). The Precambrian basement does not crop out in the Eastern Meseta domain, where the Paleozoic sequence seems to be continuous from Late Cambrian to Devonian time, being unconformably overlaid by a Visean to Westphalian flysch with limestones and volcanic rocks (Hoepffner, 1987; Michard et al., 2010b). Several Variscan and post-Variscan (330–250 Ma) granitic plutons outcrop in the Moroccan Meseta domains, intruding the Paleozoic sequences (El Hadi et al., 2006 and references therein).

The Variscan deformation that characterizes the Eastern Meseta domain is variable in style and intensity and occurred under very low- to low-grade metamorphic conditions (Hoepffner et al., 2006 and references therein). According to these authors, the deformation is generally expressed by one or more folding phases associated with a cleavage that can be penetrative or locally spaced and poorly defined. Late Variscan fault zones delineate the current boundaries between the different domains of the Moroccan Mesetas.

In the three sampled areas, the general Variscan structure consists on low- to moderate- dipping beds as a result of N-S (with variations from NW to NE) oriented upright folding and related rough axial-planar cleavage.

2.1. Oujda area

The Paleozoic sequence of the Eastern Meseta domain crops out in several relatively small areas in the Oujda region (Figs. 1B and 2), where it is characterized by Cambro-Ordovician shales, slates, minor greywackes and quartzites, dated by stratigraphic correlations with neighboring regions (Huvelin, 1970; Valin, 1979). The Silurian is characterized by black shales with Graptolites and few intercalations of thin layers of fine-grained black sandstones (Horon, 1952). The upper limit of the Silurian is not exposed in this area. The Devonian sequence is an alternation of slates, greywackes and sandstones, dated as Emsian-Frasnian with palynomorphs (Marhoumi et al., 1983). The whole Cambrian-Devonian sequence attests a general subsidence episode which was interrupted by a Late Devonian-Early Carboniferous initial Variscan deformation phase responsible for the exhumation of at least part of the Moroccan Meseta (Hoepffner, 1989). The Visean sedimentation is represented by turbidites associated with volcanic rocks (Hoepffner, 1989), whose age was assigned by facies analogy with similar deposits cropping out in the Debdou-Mekkam area palaeontologically dated by Marie (1931) and Marhoumi (1984).

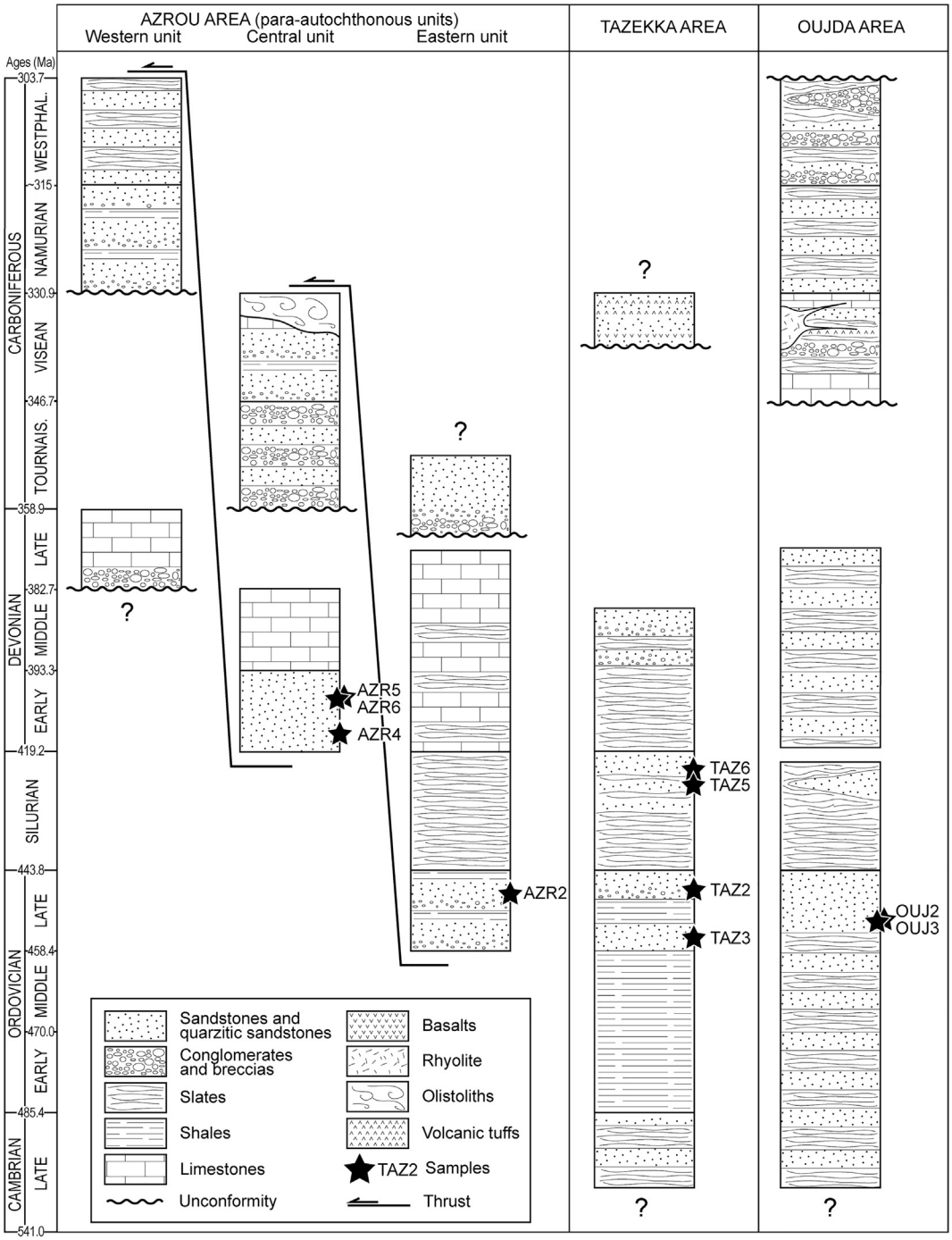

Fig. 2. Schematic correlation of the stratigraphic columns from different Paleozoic outcrops of the Eastern Meseta and Middle Atlas (not to scale): Azrou area (Bouabdelli et al., 1989 and references therein), Tazekka area (Marhoumi et al., 1989 and references therein; Vidal and Hoepffner, 1979), and Oujda area (Choubert et al., 1978; Hoepffner, 1989; Horon, 1952; Marhoumi et al., 1989).

2.2. Tazekka area

The Tazekka area is located in the northern part of the Middle Atlas, at the boundary between Eastern and Western Mesetas, corresponding with the TBBFZ (Fig. 1C). The stratigraphic sequence outcropping east of the TBBFZ is characterized by homogeneous, low-grade, intensively deformed schists (Tazekka Schists), attributed to the Devonian-Carboniferous (Hoepffner, 1987 and references therein) by facies comparison with the Debdou-Mekkam area (Mekkam Schists), where they were dated with palynomorph (Medioni, 1980) and plant fragments (Marhoumi and Rauscher, 1984). West of the TBBFZ, a less deformed and less metamorphosed Late Cambrian to Middle Devonian detrital sequence that resembles the Oujda sequence crops out (Fig. 2; Hoepffner, 1987). The sequence begins with Cambro-Ordovician slates and greywackes (dated by facies comparison with the Cambrian Paradoxides Shales of the Coastal Block; Hoepffner, 1987 and references therein), which turns upward into a thick sequence of green shales and slates dated as Lower-Middle Ordovician with fossils and palynolomorphs (Desteucq and Fournier-Vinas, 1981; Hoepffner, 1977; Rauscher et al., 1982). The Late Ordovician is characterized by sandy shales interbedded with quartzites (Tifarouine Fm.; Hoepffner, 1987; Huvelin, 1970; Khoukhi and Hamoumi, 2001; Valin, 1979), interpreted as glacial deposits (Le Heron, 2007). Similar to most of

the Moroccan Variscides outcrops, the Silurian is represented by black shales with Graptolites (Destombe, 1971), and coarser beds in the upper part of the sequence (Hoepffner, 1977), gradually passing upwards to Devonian sandstones dated with palynomorphs (Marhoumi et al., 1983).

The sedimentation appears to have been interrupted during a Late Devonian-Tournaisian tectonic phase, and then started again during the Visean, with a volcano-sedimentary succession; the age of these rocks was established by facies comparison with similar rocks cropping out in the Debdou-Mekkam area and dated by palynology (Hoepffner, 1981; Marhoumi, 1984).

2.3. Azrou area

The Azrou area (Fig. 1D) is located in the Middle Atlas, and it is characterized by the tectonic imbrication of three para-autochthonous units (Fig. 2) and an allochthonous one (Bouabdelli et al., 1989). The age of the stratigraphic sequences cropping out in these units (Ordovician to Early Carboniferous) was established by means of palynomorphs and fossil micro- and macrofaunas (Bouabdelli, 1989 and references therein).

The eastern sector corresponds to the oldest and structurally highest para-autochthonous unit, and it is characterized by a stratigraphic sequence that includes Late Ordovician sandy sediments, rarely interbedded with shales (Bouabdelli, 1982), which passes upwards to the Silurian black shales with graptolites. The Devonian sequence is characterized by alternating slates and fossiliferous Late Devonian limestones. Tournaisian quartzitic deposits lay unconformably onto the Devonian limestones.

In the central sector, the sequence is detached at the level of the Silurian shales, which are overlain by Early Devonian quartzitic and sandy slates and Middle to Upper Devonian limestones (Lazreq, 1999; Walliser et al., 2000). The sedimentation was interrupted during Late Devonian time and started again at Early Carboniferous time with the deposition of quartzitic and conglomeratic beds, passing upwards to turbiditic and gravitational deposits (Berkhli, 1999; Berkhli et al., 2000; Bouabdelli et al., 1989).

In the western sector of the Azrou area, the structurally lowest para-autochthonous unit crops out, constituted by a basal conglomerate followed by Late Devonian limestones. A Middle Carboniferous flysch and limestones with crinoids (Bouabdelli et al., 1989; Dir. Geol. Maroc, 2005; Wollen, 1974) unconformably overlay the Late Devonian succession.

The allochthonous Aït Mimoun-Bou Agri unit of Early Devonian age is characterized by turbidites passing upwards to calcarenites and calcareous reef breccias with abundant fossiliferous material (Bouabdelli et al., 1989; Dir. Geol. Maroc, 2005; Said et al., 2010).

3. Samples and methods

This study is based on the results obtained on 10 samples collected in the Late Ordovician-Early Devonian siliciclastic rocks of the Oujda, Tazekka and Azrou areas. The geographic, geological and stratigraphic locations of each sample are shown in Figs. 1 and 2, and Table 1.

OUJ2 and OUJ3 were collected 20 km westward from Oujda and they correspond to quartzites sampled in the upper part of the Ordovician sequence, just below Silurian beds of fine-grained black quartzites (according to the "Oujda" geological map scale 1:500.000; Choubert et al., 1978).

Four samples were collected close to the Tazekka National Park (Geological map "Tahala", scale 1:50.000; Vidal and Hoepffner, 1979) in the western block of the TBBFZ. Based on this geological map, samples TAZ2 and TAZ3 from Ahel Boudriss are Late Ordovician quartzites, while samples TAZ5 and TAZ6, collected 5 km south-east of Tahala, are Silurian quartzites.

Three samples (AZR4, AZR5 and AZR6) were collected 25 km south-west of Azrou, in the Sidi Bel Khair area. Based on the Geological map "Azrou" (Dir. Geol. Maroc, 2005), all of them correspond to Early Devonian quartzitic sandstones from the central para-autochthonous unit (Bouabdelli et al., 1989). Sample AZR2 was collected 5 km north-east of Azrou from the quartzitic beds of the Late Ordovician Kaâorana Formation, dated with fossiliferous material (eastern para-autochthonous unit of Bouabdelli et al., 1989; Geological map "Azrou", scale 1:50.000; Dir. Geol. Maroc, 2005).

About four kilograms of rock were collected for each sample and processed in the laboratories at the University of Granada (Spain). Samples were mechanically smashed in a jaw-crusher and sorted by sieving. A heavy mineral concentrate was obtained by manual panning. Magnetic minerals were removed from the concentrate material using a Nd magnet and, finally, about 120–160 zircon grains were separated by handpicking under a binocular microscope.

The selected zircon grains were mounted in epoxy rounds and imaged by cathodoluminescence (Fig. 3) to reveal internal structures using a Mira3 FESEM instrument at the Microscopy and Microanalysis Facility of the John de Laeter Centre (JdLC, Curtin University, Perth, Australia).

Most of the zircon grains were large enough to be analyzed with Laser Ablation Inductively Coupled Plasma Mass Spectrometry (LA-ICPMS). Where possible, 150 analyses were performed per sample in order to obtain representative and statistically significant age populations after discordant analyses were removed (Vermeesch, 2004). Fifty-six zircon grains from sample TAZ2 and 48 from TAZ3 were too small to be analyzed with LA-ICPMS, and were analyzed using the Sensitive High-Resolution Ion Microprobe (SHRIMP II) at the JdLC. Detailed analytical methods are described in the supplementary material (Appendix A).

Data with > ±10% discordance and/or > 1% ^{206}Pbc were not taken into account for results interpretation. Furthermore, SHRIMP data

Table 1
Details of the analyses carried out on the zircon grains separated from the studied samples; (*) UTM coordinates, WGS84 system, zone 30 S; (**) total analyses carried out and total concordant results (bold numbers).

Area	Sample	Location*		Lithology	Age	Zircon grains	Type of analyses	Number analyses**
		X	Y					
Oujda	OUJ2	582,303	3,834,439	Quartzite	Ordovician	123	LA-ICPMS	150/**126**
	OUJ3	582,303	3,834,439	Arkose	Ordovician	124	LA-ICPMS	150/**135**
Tazekka	TAZ2	380,945	3,774,869	Sandstone	Ordovician	79	LA-ICPMS	30/**21**
							SHRIMP	56/**44**
	TAZ3	381,775	3,773,906	Sandstone	Ordovician	92	LA-ICPMS	54/**45**
							SHRIMP	48/**41**
	TAZ5	373,058	3,765,756	Quartzite	Silurian	114	LA-ICPMS	150/**136**
	TAZ6	373,058	3,765,756	Quartzite	Silurian	126	LA-ICPMS	150/**115**
Azrou	AZR2	296,820	3,705,220	Quartzite	Late Ordovician	125	LA-ICPMS	150/**131**
	AZR4	267,866	3,692,882	Quartzite	Devonian	121	LA-ICPMS	150/**140**
	AZR5	268,951	3,692,089	Quartzite	Devonian	129	LA-ICPMS	149/**143**
	AZR6	269,001	3,690,998	Quartzite	Devonian	131	LA-ICPMS	150/**137**

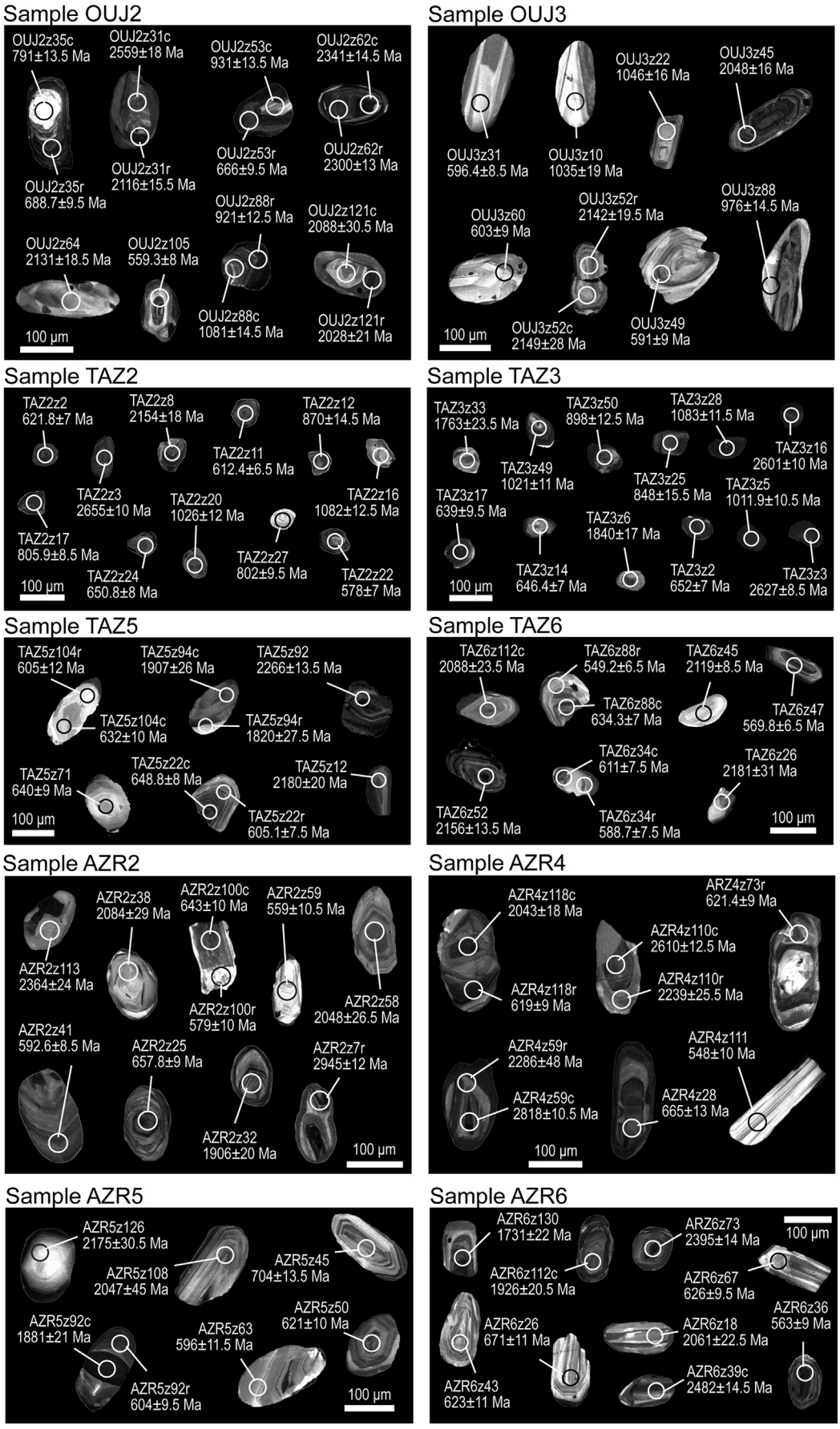

Fig. 3. Cathodoluminescence images of selected detrital zircon grains; darker zones correspond to high-U sectors and brighter zones to low-U sectors.

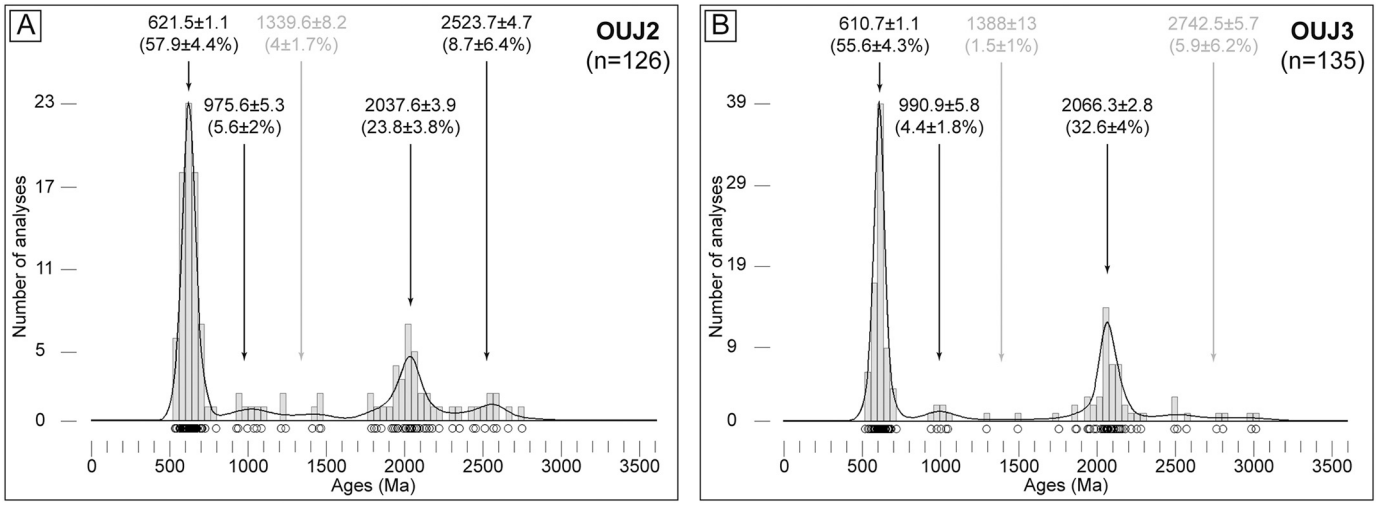

Fig. 4. Kernel Density Estimates (black lines) combined with distribution histograms (grey bars) showing the detrital zircon ages ($^{206}Pb/^{238}U$ for dates <1500 Ma; $^{207}Pb/^{206}U$ for dates >1500 Ma) obtained from the samples of the Oujda area. Errors are expressed at the 1σ level and data with a discordance level > 10% and/or > 1% ^{206}Pbc were discarded. The circles in the lowest part of the diagrams show the single analyses. The arrows indicate the main detrital zircon populations estimated using the mixture modeling tool in DensityPlotter 8.4 (Vermeesch, 2012). Grey text identifies the populations comprising scattered dates with no geological meaning. These populations were not considered in the interpretation.

were processed using the software package SQUID, which calculates the discordance percentage based on the $^{207}Pb/^{206}Pb$ and the $^{206}Pb/^{238}U$ ages corrected for common Pb. For young zircon ages, the uncertainty of $^{207}Pb/^{206}Pb$ ages is bigger due to the low content of ^{207}Pb and may produce data with high discordance level. However, when these high discordant data are plotted in a concordia diagram, they are actually concordant. $^{206}Pb/^{238}U$ dates were used to characterize zircon grains younger than 1500 Ma, and $^{207}Pb/^{206}Pb$ dates were utilized for older zircon grains. The data were plotted as combined histograms and Kernel Density Estimates (KDE) using DensityPlotter 8.4 (Vermeesch, 2012) and applying an adaptive bandwidth of 40 Ma for the KDE and a bin width of 40 Ma for the histograms (Figs. 4, 5, and 6). Detrital zircon populations were defined using the mixture modeling tool of DensityPlotter 8.4, while the mean square weighted deviation (MSWD) of the youngest populations was calculated with IsoplotR online (Vermeesch, 2018).

4. Results

A synthesis of the U-Pb analyses and estimated ages is provided in Tables 1 and 2 (the detailed analytical dataset is given in the supplementary material as Appendix B for LA-ICPMS data and Appendix C for SHRIMP data). Distribution histograms and KDE diagrams for each sample are reported in Figs. 4, 5, and 6. A description of the zircon grains of each sample (size, color, morphology, internal structure) has been included in the supplementary material as Appendix D. Because of the size of the zircon grains and/or their continuous oscillatory zoning (Fig. 3), most of the analyses were carried out only in the core of the detrital zircons; nevertheless, in some cases it was possible to analyze both the core and the rim of the grains. Errors are expressed at the 1σ level.

4.1. Oujda area

From the two samples of the Oujda area (OUJ2 and OUJ3, of Late Ordovician age), a total of 247 zircon grains were selected and 300 analyses were carried out yielding 261 concordant results.

The OUJ2 sample is a medium-grained quartzite, with muscovite and iron oxides. From this sample, 150 analyses were carried out on 123 detrital zircon grains, yielding 126 concordant data (Fig. 4A). Two main detrital zircon populations were obtained, of 529–791 Ma (Ediacaran mean age of 621.5 ± 1.1 Ma, 57.9%) and 1781–2215 Ma (Paleoproterozoic mean age of 2037.6 ± 3.9 Ma, 23.8%) ages. A few dates can be grouped into two minor and not well defined peaks: 921–1081 Ma (Tonian mean age of 975.6 ± 5.3 Ma, 5.6%) and 2300–2743 Ma (Neoarchean mean age of 2523.7 ± 4.7 Ma, 8.7%). Four scattered Mesoproterozoic data (1207–1461 Ma) cannot be grouped in a significant population. The youngest detrital zircon population, comprising 4 analyses, yielded an age of 537.5 ± 3.9 Ma (MSWD = 0.66), thus indicating an earliest Cambrian maximum depositional age.

The sample OUJ3 is a fine-grained quartzite with a faint planar fabric marked by quartz grains and opaque minerals. One hundred twenty-four detrital zircon grains were separated from this sample and a total of 150 analyses were carried out, 135 of which were concordant (Fig. 4B). The two main detrital zircon populations identified are 520–717 Ma (Ediacaran mean age of 610.7 ± 1.1 Ma, 55.6%) and 1754–2281 Ma (Paleoproterozoic mean age of 2066.3 ± 2.8 Ma, 32.6%). A few grains (941–1046 Ma) correspond to a Tonian minor peak (mean age 990.9 ± 5.8 Ma, 4.4%). A few data yield Mesoproterozoic (1293–1493 Ma) and Archean (2495–3013 Ma) ages, but they are too scattered to characterize minor populations. The youngest detrital zircon population, made up of 5 data, yielded an age of 545.3 ± 3.7 Ma (MSWD = 1.28), indicating a Late Ediacaran maximum depositional age.

In summary, detrital zircon populations of both Oujda samples are very similar and show an important Ediacaran detrital zircon population at ≈610–620 Ma, which represents ≈55–60% of the analyses. A second main peak corresponds to a Paleoproterozoic population (≈2030–2070 Ma), which represents ≈25–35% of the data. Minor detrital zircon populations yielded Tonian (≈975–990 Ma, ≈5%) and Archean (≈2520 Ma, ≈10%) ages. The maximum depositional age for both samples is Late Ediacaran - Early Cambrian (≈540 Ma).

4.2. Tazekka area

A total of 411 zircon grains were isolated from the 4 samples of the Tazekka area: TAZ2 and TAZ3, of Late Ordovician age, and TAZ5 and TAZ6, of Silurian age. A total of 488 analyses were carried out (104 with SHRIMP in samples TAZ2 and TAZ3) yielding 402 concordant results (86 with SHRIMP in samples TAZ2 and TAZ3).

Sample TAZ2 is a very fine-grained quartzite with some detrital micas. From this sample, 79 zircon grains were separated and 86 analyses were carried out, 65 of which gave concordant ages (21 LA-ICPMS and 44 SHRIMP analyses, see Table B.3 in Appendix B and Table C.1 in Appendix C). Concordant LA-ICPMS and SHRIMP data were then

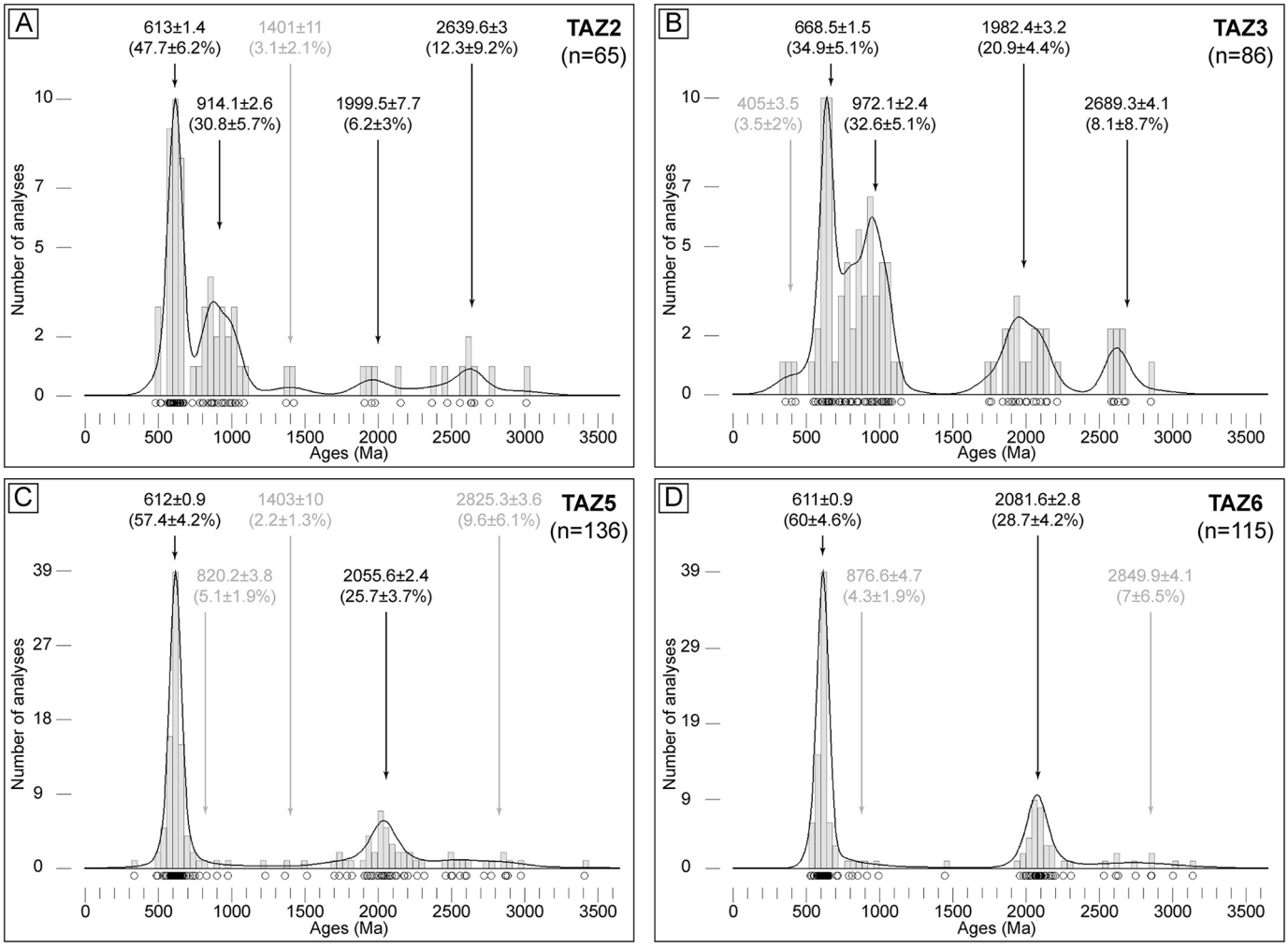

Fig. 5. Kernel Density Estimates (black lines) combined with distribution histograms (grey bars) showing the detrital zircon ages ($^{206}Pb/^{238}U$ for dates <1500 Ma; $^{207}Pb/^{206}U$ for dates >1500 Ma) obtained from the samples of the Tazekka area. Errors are expressed at the 1σ level and data with a discordance level > 10% and/or > 1% ^{206}Pbc were discarded. The circles in the lowest part of the diagrams show the single analyses. The arrows indicate the main detrital zircon populations estimated using the mixture modeling tool in DensityPlotter 8.4 (Vermeesch, 2012). Grey text identifies the populations comprising scattered dates with no geological meaning. These populations were not considered in the interpretation.

combined to create the histogram and KDE shown in Fig. 5A. The main detrital zircon populations are 480–674 Ma (Ediacaran mean age of 613 ± 1.4 Ma, 47.7%) and 731–1082 Ma (Tonian mean age of 914.1 ± 2.6 Ma, 30.8%). Minor populations in this sample are 1908–2154 Ma (Paleoproterozoic mean age of 1999.5 ± 7.7 Ma, 6.2%) and 2369–3012 Ma (Archean mean age of 2639.6 ± 3 Ma, 12.3%). Two data yield Mesoproterozoic ages (1373–1425 Ma). The youngest detrital zircon population, made up of 8 grains, gave an age of 581.4 ± 2.8 Ma (MSWD = 0.53), indicating a Late Ediacaran maximum depositional age.

Sample TAZ3 corresponds to a quarzitic sandstone. Its grain size is very fine and homogeneous, quartz crystals being rounded and with no preferential orientation. 92 grains were separated from sample TAZ3, and 102 analyses were carried out yielding 86 concordant dates (45 LA-ICPMS and 41 SHRIMP analyses, see Table B.4 in Appendix B and Table C.2 in Appendix C). Concordant SHRIMP and LA-ICPMS data were used to generate the histogram and the KDE curve showed in Fig. 5B. The main detrital zircon populations are 547–803 Ma (Cryogenian mean age of 668.5 ± 1.5 Ma, 34.9%) and 813–1146 Ma (Tonian mean age of 972.1 ± 2.4 Ma, 32.6%). Paleoproterozoic (1746–2211 Ma, mean age 1982.4 ± 3.2 Ma, 20.9%) and Archean (2583–2851 Ma, mean age 2689.3 ± 4.1 Ma, 8.1%) peaks represent minor populations. Three scattered data gave Late Silurian-Devonian ages (426, 399, and 359 Ma), which will not be considered to establish the maximum depositional age. Thus, the youngest detrital zircon population, composed of 4 concordant analyses, yielded an age of 607.6 ± 3.5 Ma (MSWD = 0.34), indicating an Ediacaran maximum depositional age.

Sample TAZ5 is a medium- to coarse-grained quartzite. The quartz grains are rounded and do not show any preferential shape orientation. From this sample 114 zircon grains were handpicked and a total of 150 analyses were performed, yielding 136 concordant results (Fig. 5C). The main detrital zircon population is 488–750 Ma (Ediacaran mean age of 612 ± 0.87 Ma, 57.4%); a Paleoproterozoic (1702–2316 Ma, mean age 2055.6 ± 2.4 Ma, 25.7%) peak represents a minor detrital zircon population. Scattered data gave Tonian (782–977 Ma), Mesoproterozoic (1231–1513 Ma) and Siderian-Archean ages (2460–3407 Ma). The youngest population, comprising 5 grains, yielded an age of 554.2 ± 3 Ma (MSWD = 0.77), indicating a Late Ediacaran maximum depositional age.

Sample TAZ6 is a medium-grained quartzite with equidimensional quartz grains and some small mica grains. 126 zircons were separated from this sample and 150 analyses were carried out, yielding 115 concordant ages (Fig. 5D). The two main detrital zircon populations are 527–714 Ma (Ediacaran mean age of 611.04 ± 0.92 Ma, 60%) and 1955–2304 Ma (Paleoproterozoic mean age of 2081.6 ± 2.8 Ma, 28.7%). A few, very scattered data yielded Tonian (787–992 Ma), Mesoproterozoic (1442 ± 17.5 Ma), and Archean (2528–3135 Ma)

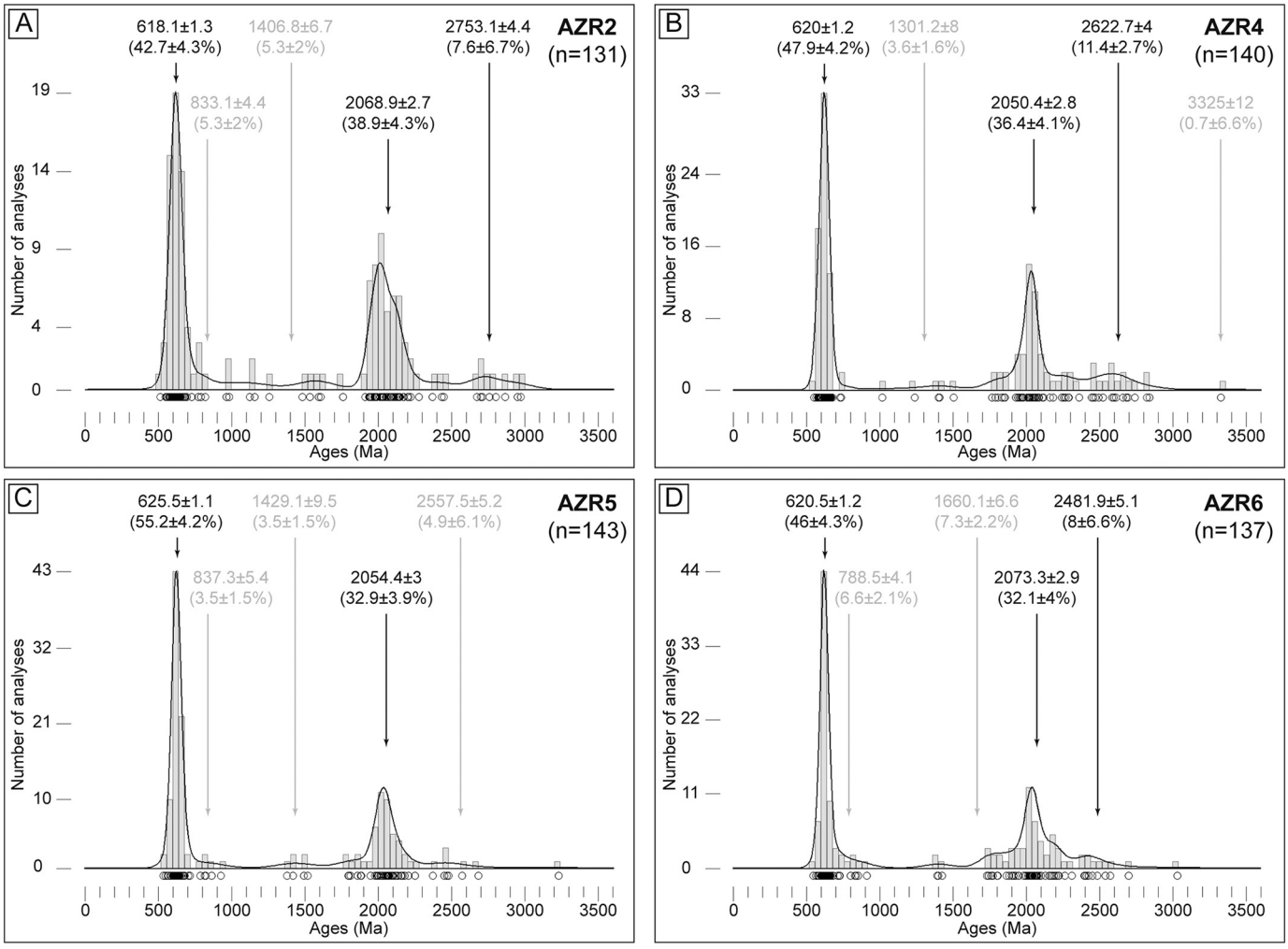

Fig. 6. Kernel Density Estimates (black lines) combined with distribution histograms (grey bars) showing the detrital zircon ages ($^{206}Pb/^{238}U$ for dates <1500 Ma; $^{207}Pb/^{206}U$ for dates >1500 Ma) obtained from the samples of the Azrou areas. Errors are expressed at the 1σ level and data with a discordance level > 10% and/or > 1% ^{206}Pbc were discarded. The circles in the lowest part of the diagrams show the single analyses. The arrows indicate the main detrital zircon populations estimated using the mixture modeling tool in DensityPlotter 8.4 (Vermeesch, 2012). Grey text identifies the populations comprising scattered dates with no geological meaning. These populations were not considered in the interpretation.

ages. The youngest detrital zircon population, made up of 10 analyses, yielded an age of 579.7 ± 2.3 Ma (MSWD = 0.95), indicating a Late Ediacaran maximum depositional age.

To sum up, all samples from the Tazzeka area are characterized by a main Ediacaran-Cryogenian detrital zircon population (≈610–670 Ma, ≈35–60%) and a minor Paleoproterozoic peak (≈1980–2080 Ma, ≈5–30%). Nevertheless, in samples TAZ2 and TAZ3 an important Tonian population (≈915–975 Ma, ≈30%) and a secondary Archean peak (≈2640–2690 Ma, ≈10–15%) are observed. The maximum depositional ages are Ediacaran (≈555–605 Ma).

4.3. Azrou area

Of the 506 zircon grains isolated from the 4 samples of the Azrou area (AZR2, Late Ordovician age; AZR4, AZR5, and AZR6, Early Devonian

Table 2
Details of the different detrital zircon populations in the analyzed samples; errors are expressed at the 1σ level; N°: number of grains in the youngest population.

Area	Sample	Youngest zircon population		Youngest zircon age (Ma)	Ediacaran-Cryogenian		Tonian-Stenian		Paleoproterozoic		Archean	
		age (Ma)	N°		Age (Ma)	Prob. (%)	Age (Ma)	Prob. (%)	Age (Ma)	Prob. (%)	Age (Ma)	Prob. (%)
Oujda	OUJ2	537.5 ± 3.9	4	529 ± 8.5	621.5 ± 1.1	57.9	975.6 ± 5.3	5.6	2037.6 ± 3.9	23.8	2523.7 ± 4.7	8.7
	OUJ3	545.3 ± 3.7	5	520 ± 10	610.7 ± 1.1	55.6	990.9 ± 5.8	4.4	2066.3 ± 2.8	32.6	–	–
Tazekka	TAZ2	581.4 ± 2.8	8	480 ± 6	613 ± 1.4	47.7	914.1 ± 2.6	30.8	1999.5 ± 7.7	6.2	2639.6 ± 3	12.3
	TAZ3	607.5 ± 3.5	4	339 ± 6	668.5 ± 1.5	34.9	972.1 ± 2.4	32.6	1982.4 ± 3.2	20.9	2689.3 ± 4.1	8.1
	TAZ5	554.2 ± 3	5	336 ± 5.5	612 ± 0.9	57.4	–	–	2055.6 ± 2.4	25.7	–	–
	TAZ6	579.7 ± 2.3	10	527.4 ± 7	611 ± 0.9	60	–	–	2081.6 ± 2.8	28.7	–	–
Azrou	AZR2	570 ± 3.5	8	511.8 ± 7.5	618.1 ± 1.3	42.7	–	–	2068.9 ± 2.7	38.9	2753.1 ± 4.4	7.6
	AZR4	591 ± 2	21	548 ± 10	620 ± 1.2	47.9	–	–	2050.4 ± 2.8	36.4	2622.7 ± 4	11.4
	AZR5	612 ± 2	41	532 ± 8.5	625.5 ± 1.1	55.2	–	–	2054.4 ± 3	32.9	–	–
	AZR6	577 ± 8	4	545.3 ± 8	620.5 ± 1.2	46	–	–	2073.3 ± 2.9	32.1	2481.9 ± 5.1	8

age), a total of 597 analyses were carried out, yielding 555 concordant ages.

Sample AZR2 is a medium- to fine-grained quartzite with rare detrital micas and a very faint preferential shape orientation of the quartz grains. From this sample 125 zircon grains were separated and 150 analyses yielded 131 concordant dates (Fig. 6A). The main detrital zircon populations are 511–725 Ma (Ediacaran mean age of 618.1 ± 1.3 Ma, 42.7%) and 1906–2273 Ma (Paleoproterozoic mean age of 2068.9 ± 2.7 Ma, 38.9%), while ages in the range 2364–2966 Ma (Archean mean age of 2753.1 ± 4.4 Ma, 7.6%) represent a third minor population. A few scattered data yielded Tonian-Stenian (769–1154 Ma) and Mesoproterozoic (1253–1756 Ma) ages. The youngest detrital zircon population, made up of 8 analyses, yielded an age of 570 ± 3.5 Ma (MSWD = 1.10), indicating a Late Ediacaran maximum depositional age.

Sample AZR4 corresponds to a medium-grained quartzite with rounded grains that do not define any planar fabric. A total of 150 analyses were carried out on 121 zircon grains separated from this sample. One hundred and forty of the analyses gave concordant results (Fig. 6B). A 548–733 Ma population (Ediacaran mean age of 620 ± 1.2 Ma, 47.9%) marks the principal peak in this sample; minor populations yielded 1762–2358 Ma (Paleoproterozoic mean age of 2050.4 ± 2.8 Ma, 36.4%) and 2441–2838 Ma (Archean mean age of 2622.7 ± 4 Ma, 11.4%) ages. A few data, too scattered to be considered as minor populations, gave Mesoproterozoic (1012–1500 Ma) and Paleoarchean (3325 ± 12 Ma) ages. The youngest detrital zircon population, made up of 21 analyses, yielded an age of 591 ± 2 Ma (MSWD = 1.03), indicating an Ediacaran maximum depositional age.

Sample AZR5 is a homogeneous medium-grained quartzite, with a few opaque minerals filling fractures and very scarce micas. From this sample 129 zircon grains were handpicked, 149 analyses were performed, yielding 143 concordant ages (Fig. 6C). Fifty-five percent of the data correspond to the age range 532–716 Ma (Ediacaran mean age of 625.5 ± 1.1 Ma), while 32.9% define a Paleoproterozoic age (1793–2267 Ma, mean age 2054.4 ± 3 Ma). A few scattered data yielded Tonian (786–926 Ma), Mesoproterozoic (1374–1517 Ma), and Archean (2367–3225 Ma) ages. The youngest zircon population, made up of 41 data, gave an age of 612 ± 2 Ma (MSWD = 1.3), indicating an Ediacaran maximum depositional age.

Finally, sample AZR6 is a quartzite very similar to samples AZR4 and AZR5. The grain size is medium and homogeneous and there is no evidence of preferential shape quartz orientation. 131 zircon grains were separated from this sample and 150 analyses were carried out, yielding 137 concordant dates (Fig. 6D). The 545–726 Ma detrital zircon population (Ediacaran mean age of 620.5 ± 1.2 Ma, 46%) represents the highest peak in this sample; a second population yielded a Paleoproterozoic age (1729–2308 Ma, mean age 2073.3 ± 2.9 Ma, 32.1%), while a third minor peak represents a Siderian population (2395–2572 Ma, mean age 2481.9 ± 5.1 Ma, 8%). A few scattered data yielded Tonian (798–910 Ma), Mesoproterozoic (1389–1424 Ma), and Archean (2699–3029 Ma) ages. The youngest population, composed of 4 analyses, gave an age of 577 ± 8 Ma (MSWD = 1.3), indicating a Late Ediacaran maximum depositional age.

In summary, the most prominent feature of the Azrou samples is the Ediacaran peak at ≈620 Ma, which represents the ≈40–55% of the results. The Paleoproterozoic population (≈2050–2080 Ma) is well defined and represents ≈30–40% of the data. A third minor peak (≈5–10%) corresponds to an Archean population at ≈2480–2750 Ma. The maximum depositional age for these samples is Ediacaran (≈570–615 Ma).

5. Discussion

5.1. Maximum depositional ages and stratigraphic attributions

The age of the youngest detrital zircon population is often used to constrain the maximum depositional age of the sample. In this study, all the samples yielded (earliest Cambrian-) Ediacaran ages for the youngest zircon populations (Table 2). Specifically, the Ordovician samples OUJ2 and OUJ3 from the Oujda area gave a youngest detrital zircon population age of ≈540 Ma, while the Late Ordovician-Devonian samples from Azrou area yielded youngest zircon populations with variable ages between ≈570 and 610 Ma; finally, the samples from the Tazekka area (TAZ2 and TAZ3, Ordovician; TAZ5 and TAZ6, Silurian) gave maximum depositional ages of ≈555–605 Ma. Therefore, our data are compatible with the previous stratigraphic attribution of these samples, since the maximum depositional age is in all cases older than the putative stratigraphic age. Regarding the reliability of the stratigraphic ages of the different formations sampled in this work, it must be noticed that in a few cases those ages are based on previously reported fossiliferous content, though in most cases they rely on regional stratigraphic correlations of analogous passive margin sequences (see Section 2). Furthermore, an Ediacaran age attribution can be discarded by considering that the rocks of that age locally cropping out in the Moroccan Meseta are quite different from the Paleozoic rocks: they consist on felsic volcanic and volcanoclastic rocks with granitoids, all of them probably attesting a Cadomian magmatic arc bordering northern Gondwana at that time (Eddif et al., 2007; El Houicha et al., 2018; Letsch et al., 2018; Ouabid et al., 2017; Tahiri et al., 2010). The consistent Ediacaran maximum depositional age of our samples simply reflects that the magmatism of that age generated the youngest zircons incorporated as detrital material into these Ordovician to Devonian rocks (see next subsections).

5.2. West African Craton provenance

Most of the U-Pb geochronological results published so far in detrital rocks from the Moroccan Variscides (*e.g.* Abati et al., 2010; Avigad et al., 2012; Domènech et al., 2018; El Houicha et al., 2018; Ghienne et al., 2018; Letsch et al., 2018; Marzoli et al., 2017; Pérez-Cáceres et al., 2017; Pratt et al., 2015) are characterized by Ediacaran-Cryogenian and Paleoproterozoic detrital zircon populations, with a significant gap at Mesoproterozoic ages. Such characteristics are considered the typical signature of WAC affinity (Fig. 7), the main detrital zircon populations being attributed to the Cadomian and/or Pan-African (Ediacaran-Cryogenian) and Eburnean (Paleoproterozoic) orogenies (Nance et al., 2008 and references therein). An Archean population, possibly attributed to the Liberian orogeny (Nance et al., 2008 and references therein), is often present but at very scarce percentages. The absence of relevant Mesoproterozoic populations strongly suggests that the source of the zircons of that age described by Bradley et al. (2015) in Ediacaran samples directly overlying the western WAC in Mauritania should be located in a more westerner area, *i.e.* an Amazonian basement.

All the samples described in this work include the above-mentioned WAC-diagnostic three detrital zircon populations (Ediacaran-Cryogenian, Paleoproterozoic, and Archean). In particular, the Late Ordovician-Early Devonian samples from the Azrou area (AZR2, AZR4, AZR5, and AZR6) and the two Silurian samples from the Tazekka area (TAZ5 and TAZ6) are characterized by a strong WAC affinity, their detrital zircon content being comparable with previously published studies in the region (*e.g.* Abati et al., 2010; Avigad et al., 2012; Domènech et al., 2018; El Houicha et al., 2018; Ghienne et al., 2018; Letsch et al., 2018; Marzoli et al., 2017; Pérez-Cáceres et al., 2017; Pratt et al., 2015). For this reason, and because of the similarities in the Early Paleozoic stratigraphic record within the Moroccan Variscides (Michard et al., 2010b and references therein), it seems plausible that the Moroccan Meseta domains were all part of the same continental margin located to the north of the WAC (*i.e.* at the northern margin of the Gondwanan continent). In fact, a WAC-type basement locally crops out in the Western Moroccan Meseta: besides Cadomian rocks (see Section 5.1), an Eburnean (≈2.05 Ga) meta-rhyolite has been described covered by Lower Cambrian sedimentary rocks (Pereira et al., 2015). This Moroccan Meseta Precambrian basement, if exposed during the

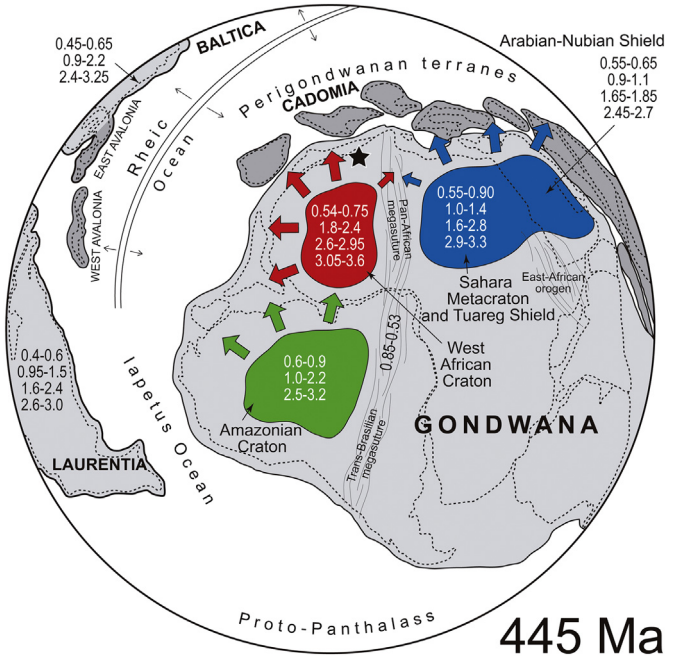

Fig. 7. Palinspastic reconstruction of Gondwana, Laurentia, and Baltica (light grey) and Peri-Gondwanan terranes (dark grey) during Late Ordovician (about 445 Ma; modified from Bea et al., 2010; Linnemann et al., 2011; Naidoo et al., 2018). Ages are from Abati et al. (2010), Bea et al. (2010), Linnemann et al. (2011 and references therein), Naidoo et al. (2018), and Nance et al. (2008), and they are expressed in Ga. Colored arrows indicate the main transport directions of the sediments from the source areas within the northwestern Gondwanan continent. The black star indicates the approximate location of the area studied.

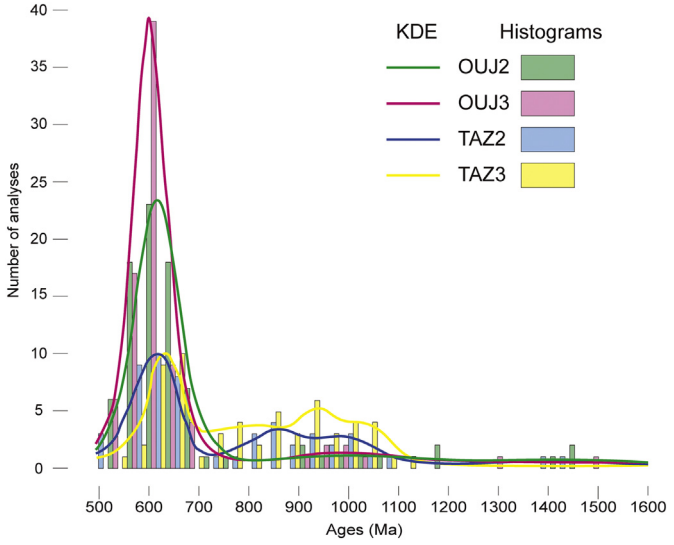

Fig. 8. Summary Kernel Density Estimator (KDE, lines) and histograms (bars) combination of samples OUJ2 ($n = 85$ of 126, in green), OUJ3 ($n = 83$ of 135, in red), TAZ2 ($n = 53$ of 65, in blue) and TAZ3 ($n = 59$ of 88, in yellow) showing the different distribution patterns of data in the age range from 450 to 1600 Ma. (For interpretation of the references to color in this figure legend, the reader is referred to the web version of this article.)

Ordovician-Devonian, could have been and additional local source for the Ediacaran and Paleoproterozoic zircon grains of our samples.

5.3. Tonian-Stenian population

Although all the samples show a dominant WAC affinity, the detrital zircon distribution patterns of a few of them diverge from the classical WAC signature, with secondary or minor detrital zircon populations of Tonian-Stenian age (Fig. 8). In particular, the Late Ordovician samples from the Oujda area (OUJ2 and OUJ3) and the Late Ordovician samples from the Tazekka area (TAZ2 and TAZ3) include a Tonian-Stenian (about 1.0 Ga) population which reaches 30% of the analyses in the samples from Tazekka. Primary sources of that age are unknown in the WAC, but they are typical of the Grenville orogeny which affected Laurentia, Baltica, Avalonia, and the Amazonian Craton (Fig. 7; Slagstad et al., 2017 and references therein), as well as the Arabian-Nubian shield and the Saharan Metacraton. Furthermore, because of the very small dimensions of the grains and their rounded morphology (particularly evident in samples TAZ2 and TAZ3; Fig. 3), these zircons probably went through several cycles of erosion, transportation, and deposition, being finally deposited during the Late Ordovician glaciation that affected northern Gondwana (Ghienne et al., 2018; Le Heron et al., 2009). Consequently, it is possible that the Tonian-Stenian zircon grains analyzed in this work hailed from distant source areas that might be thousands of kilometers away from the current location of the sample sites.

Laurentia, Baltica and Avalonian sources can be dismissed because they were separated from Gondwana by the Rheic Ocean at Ordovician to Late Devonian times (Fig. 7). On the contrary, the Amazonian Craton was part of the Gondwana continent and it might be a plausible source area. However, zircon ages from this craton are continuous during all the Mesoproterozoic (1.0–1.6 Ga, and up to 2.2 Ga, Fig. 7). Therefore, we would expect to find an analogous age pattern in detrital samples (Fig. 9A) sourced from an Amazonian-type basement (for instance, the zircons described in Bradley et al., 2015), but our samples only contain a few scattered Early to Middle Mesoproterozoic zircon grains (Fig. 9B), thus suggesting a different source area. Actually, a more plausible source for the 1.0 Ga detrital zircons might be the Saharan Metacraton and/or the Arabian-Nubian Shield, which also contain zircons of that age (Fig. 7). In this regard, northeastern African igneous sources were already suggested to explain the presence of Tonian-Stenian detrital zircon populations in samples from central and northern Iberia (Bea et al., 2010; Fernández-Suárez et al., 2014; Gutiérrez-Alonso et al., 2015; Pastor-Galán et al., 2013; Shaw et al., 2014; Talavera et al., 2012). Furthermore, such sources were previously claimed to explain minor Tonian-Stenian detrital zircon populations in samples from the Anti-Atlas (Avigad et al., 2012), High Atlas (Marzoli et al., 2017), and Middle Atlas (Ghienne et al., 2018; Pratt et al., 2015). However, Marzoli et al. (2017) and Pratt et al. (2015) studied post-Variscan rocks, which hampers provenance investigations because continental terranes with 1.0 Ga primary sources (*e.g.* Avalonia, Baltica and Laurentia) were already amalgamated with Gondwana at the time of deposition of the studied samples. Accordingly, the above-mentioned authors proposed northeastern African sources as well as Amazonian or Avalonian provenance areas. However, the continuous Mesoproterozoic age distribution patterns in the Avalonian and Amazonian areas, in contrast to the pattern observed in the Moroccan samples (Fig. 9), remains, in our opinion, the strongest point in favour of northeastern African sources. For the same reason, Ghienne et al. (2018) discarded the Amazonian Craton as a source area for Tonian-Stenian detrital zircons in the Tazekka area. According to these authors, 1.0 Ga grains in this area are found in sedimentary rocks deposited during a glacial maximum, making it possible that glaciers enhanced the transportation of detrital zircon grains from the northeastern regions of Africa (Saharan Metacraton and Arabian-Nubian Shield; Fig. 7) to the Tazekka glacial depocenter. In this regard, the Ordovician age of samples OUJ2, OUJ3, TAZ2, and TAZ3 suggests that similar processes might be responsible for the accumulation of a Tonian-Stenian detrital zircon population in our samples.

Apart from the possibility of a very distant NE African source, it is possible that during the Ordovician, the Eastern Meseta was located in a closer position to the 1.0 Ga zircon sources of NE Africa. In this case, important regional faults, such as the SMF, would be necessary to explain the current position of the Eastern Meseta. Nevertheless, the

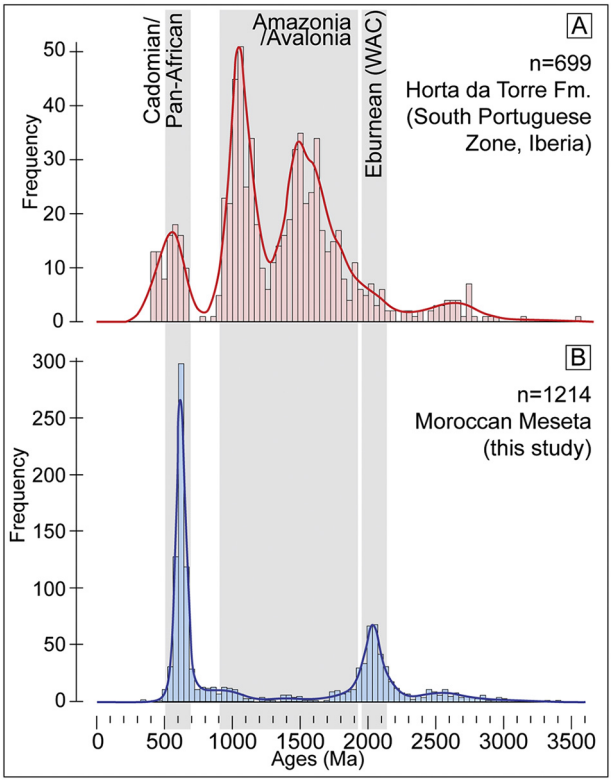

Fig. 9. Comparison between Kernel Density Estimator (KDE) and histograms of U-Pb detrital zircon concordant ages: (A) data from the Devonian quartzites of the Horta da Torre Formation (Pulo do Lobo unit, South Portuguese Zone, SW Variscan Iberian Massif (Fig. 1A); data compiled from Braid et al. (2011) and Pérez-Cáceres et al. (2017)), considered a typical example of Avalonian/Amazonian-derived sediments; (B) our data from the Eastern Meseta and Middle Atlas. Grey areas indicate the main crustal growth events in northern Gondwana.

SMF is characterized by dextral transpressional kinematics (Cerrina Feroni et al., 2010; Michard et al., 2010b), which is not congruent with the type of displacement needed to move the studied terranes from an original eastern position to their present day location. Moreover, the age and kinematic history of this structure is still a matter of discussion (Michard et al., 2010a; Simancas et al., 2009, 2010).

To conclude, the deposition of Tonian-Stenian detrital zircon grains probably occurred through long-travelled transportation from northeastern Africa, enhanced by Ordovician glaciation, and/or involving several cycles of erosion, transportation and sedimentation.

5.4. Cambro-Ordovician rifting in northern Gondwana

After the Ediacaran Cadomian subduction, the northern border of Gondwana was dominated, during the Early Paleozoic, by a rifting episode that preceded the opening of the Rheic Ocean (*e.g.* Cambeses et al., 2017; Nance et al., 2010, 2012). Continental rift features, including very thick Cambrian and Ordovician sedimentary accumulations (up to 10 km) and copious Cambro-Ordovician rift-related plutonic and volcanic rocks (and the detrital zircon populations derived from them), are common in Variscan terranes now cropping out in central and southern Europe (*e.g.* Cambeses et al., 2017; Demange, 1994; Linnemann et al., 2008 and references therein; Montero et al., 2009; Pastor-Galán et al., 2013; Pereira et al., 2012 and references therein; Pérez-Estaún et al., 1990).

In the Moroccan Meseta, evidence of Lower Paleozoic rifting is rather restricted in space and time. Sedimentary *grabens* have only been documented in the Middle Cambrian of the Coastal Block (Bernardin et al., 1988). Magmatic rocks are represented by discrete lenses of Cambrian mafic volcanics in the Coastal Block and rarely in the Central zone of the Western Moroccan Meseta (Pouclet et al., 2018 and references therein). Cambro-Ordovician detrital zircon populations are almost missing, with the exception of a narrow unimodal zircon population centered at around 488 Ma recognized by Letsch et al. (2018) in a Lower Paleozoic greywacke from the Western Moroccan Meseta. A few Cambro-Ordovician detrital zircon ages were also obtained in Late Ordovician sandstones (Ghienne et al., 2018) and in Middle Jurassic sandstones (Pratt et al., 2015) from the Middle Atlas. As shown in Figs. 4, 5, and 6, no Cambro-Ordovician detrital zircon populations were found in any of our samples from the Eastern Moroccan Meseta and Middle Atlas.

Based on the extent of the rift-related magmatism and detrital zircon content in Ordovician-Devonian rocks, it is generally accepted that Cambro-Ordovician rifting widely affected northern Gondwana-derived terranes, which are now exposed in Variscan massifs of central and southern Europe (*e.g.* Cambeses et al., 2017; Linnemann et al., 2008; Montero et al., 2009; Pereira et al., 2012). Regarding the Moroccan Mesetas, we propose that Early Paleozoic rifting, accompanied by magmatism, partially affected the Western Meseta and aborted soon in late Cambrian time, but had no influence on the Eastern Meseta. Therefore, we suggest that the latter was located in a more inland position than the Western Meseta, and far from the rifted continental margin affected by rift-related magmatism (Iberia and central Europe correlatives).

6. Conclusions

The detrital zircon U-Pb dates obtained on Ordovician-Devonian rocks of the Eastern Moroccan Meseta (Oujda area) and Middle Atlas (Tazekka and Azrou areas) are similar to those obtained on other samples from the Western Meseta, attesting a strong WAC affinity, characterized by Ediacaran-Cryogenian, Paleoproterozoic, and minor Archean populations. Despite these similarities, it is worth highlighting that the samples studied in this work did not record Cambro-Ordovician magmatism (rifting phase preceding the opening of the Rheic Ocean that allowed the drift of peri-Gondwanan terranes). Such magmatism is locally evidenced in the Western Meseta, and widespread in southwestern Europe. This suggests that the Eastern Moroccan Meseta (and to some extent the Western Meseta) was located in northern Gondwana, relatively far from the portion of the continental margin affected by the rifting pulse.

The Late Ordovician samples from the Tazekka area and, to a lesser extent, the samples from the Oujda area, show an important (up to 30% of the data) Tonian-Stenian population which suggests the presence of exotic sources apart from the WAC, probably located in northeastern Africa (Saharan Metacraton and Arabian-Nubian Shield). The presence of this population in Ordovician samples from northwestern Africa sequences might be explained by the glaciation that occurred during the Late Ordovician in northern Gondwana. Furthermore, the small size and rounded morphology of the grains suggest that they experienced significant sedimentary recycling.

Acknowledgements

This study was funded by the Ministerio de Economía y Competividad (MINECO) of Spain through the project CGL2015-71692-P and the Pre-Doctoral scholarship BES-2016-078168. Zircon analyses and imaging were carried out on the SHRIMP II, LA-ICPMS and SEM facilities at the John de Laeter Centre, Curtin University, with the financial support of the Australian Research Council (LE150100013) and Auscope NCRIS (AQ44 Australian Education Investment Fund program). The authors wish to thank Brad McDonald (Curtin University) for technical assistance regarding LA-ICPMS analyses, and Lorenzo Valetti for proof reading the manuscript. Constructive comments by two anonymous reviewers are greatly appreciated and helped to improve the manuscript.

Appendices. Supplementary data

Supplementary data to this article can be found online at https://doi.org/10.1016/j.lithos.2019.04.011.

References

Abati, J., Mohsine Aghzer, A., Gerdes, A., Ennih, N., 2010. Detrital zircon ages of Neoproterozoic sequences of the Moroccan Anti-Atlas belt. Precambrian Res. 181, 115–128. https://doi.org/10.1016/j.precamres.2010.05.018.

Avigad, D., Gerdes, A., Morag, N., Bechstädt, T., 2012. Coupled U-Pb-Hf of detrital zircons of Cambrian sandstones from Morocco and Sardinia: implications for provenance and Precambrian crustal evolution of North Africa. Gondwana Res. 21, 690–703. https://doi.org/10.1016/j.gr.2011.06.005.

Avigad, D., Kolodner, K., McWilliams, M., Persing, H., Weissbrod, T., 2003. Origin of northern Gondwana Cambrian sandstone revealed by detrital zircon SHRIMP dating. Geology 31, 227. https://doi.org/10.1130/0091-7613(2003)031<0227:OONGCS>2.0.CO;2.

Bea, F., Montero, P., Talavera, C., Abu Anbar, M., Scarrow, J.H., Molina, J.F., Moreno, J.A., 2010. The palaeogeographic position of Central Iberia in Gondwana during the Ordovician: evidence from zircon chronology and Nd isotopes. Terra Nova 22, 341–346. https://doi.org/10.1111/j.1365-3121.2010.00957.x.

Berkhli, M., 1999. Sédimentologie, biostratigraphie et stratigraphie séquentielle du Nord-Est de la Méséta occidentale marocaine pendant le Carbonifère inférieur (Viséen-Serpoukhovien). Université Moulay-Ismaïl, Meknès, Maroc.

Berkhli, M., Vachard, D., Paicheler, J.-C., Tahiri, A., 2000. Modèle sédimentaire et évolution géodynamique du Nord-Est de la Méséta occidentale marocaine au cours du Carbonifère inférieur. C. R. Acad. Sci. Ser. IIA Earth Planet. Sci. 331, 251–256. https://doi.org/10.1016/S1251-8050(00)01417-8.

Bernardin, C., Cornée, J.J., Corsini, M., Mayol, S., Muller, J., Tayebi, M., 1988. Variations d'épaisseur du Cambrien moyen en Meseta marocaine occidentale: signification géodynamique des données de surface et de subsurface. Can. J. Earth Sci. 25, 2104–2117.

Bouabdelli, M., 1982. Stratigraphie et évolution structurale du Paléozoïque d'Azrou. Université Louis Pasteur, Strasbourg.

Bouabdelli, M., 1989. Tectoniaue et sédimentation dans un bassin orogénique : le sillon viseén d'Azrou-Khénifra (est du Massif Hercynien Central du Maroc). Université Louis Pasteur, Strasbourg.

Bouabdelli, M., Cailleux, Y., Hoepffner, C., Michard, A., Pique, A., 1989. Le bassin dinantien d'Azrou et l'évolution de sa déformation hercynienne (Méséta marocaine nord-orientale). Notes Mém. Serv. Géol. Maroc 335, 221–227.

Bradley, D.C., O'Sullivan, P., Cosca, M.A., Motts, H.A., Horton, J.D., Taylor, C.D., Beaudoin, G., Lee, G.K., Ramezani, J., Bradley, D.B., Jones, J.V., Bowring, S., 2015. Synthesis of geological, structural, and geochronologic data (phase V, deliverable 53). In: Taylor, C.D. (Ed.), Second Projet de Renforcement Institutionnel Du Secteur Minier de La République Islamique de Mauritanie (PRISM-II): U.S. Geological Survey Open-File Report 2013–1280-A, p. 328 https://doi.org/10.3133/ofr20131280.

Braid, J.A., Murphy, J.B., Quesada, C., Mortensen, J., 2011. Tectonic escape of a crustal fragment during the closure of the Rheic Ocean: U-Pb detrital zircon data from the Late Palaeozoic Pulo de Lobo and South Portuguese Zones, Southern Iberia. J. Geol. Soc. Lond. 168, 383–392. https://doi.org/10.1144/0016-76492010-104.

Cambeses, A., Scarrow, J.H., Montero, P., Lázaro, C., Bea, F., 2017. Palaeogeography and crustal evolution of the Ossa–Morena Zone, southwest Iberia, and the North Gondwana margin during the Cambro-Ordovician: a review of isotopic evidence. Int. Geol. Rev. 59, 94–130. https://doi.org/10.1080/00206814.2016.1219279.

Cerrina Feroni, A., Ellero, A., Malusà, M.G., Musumeci, G., Ottria, G., Polino, R., Leoni, L., 2010. Transpressional tectonics and nappe stacking along the Southern Variscan front of Morocco. Int. J. Earth Sci. 99, 1111–1122. https://doi.org/10.1007/s00531-009-0449-x.

Chopin, F., Corsini, M., Schulmann, K., El Houicha, M., Ghienne, J.-F., Edel, J.-B., 2014. Tectonic evolution of the Rehamna metamorphic dome (Morocco) in the context of the Alleghanian-Variscan orogeny. Tectonics 33, 1154–1177. https://doi.org/10.1002/2014TC003539.

Choubert, G., Marçais, J., Suter, G., 1978. Carte géologique du Maroc - 1/500.000: Oujda. Royaume du Maroc, Ministère l'Énergie des Mines du Développement Durable.

Demange, M., 1994. Antevariscan evolution of the Montagne Noire (France): from a passive margin to a foreland basin. 318. Comptes Rendus l'Académie des Science de Paris, pp. 921–933.

Desteucq, C., Fournier-Vinas, C., 1981. Présence d'Ordovicien dans la région d'Oujda. Mines, Géologie et Énergie 50.

Destombe, J., 1971. L'Ordovicien au Maroc. Essai de synthèse stratigraphique. Mémoires du Bureau de Recherches Géologiques et Minières 73. pp. 237–263.

Maroc, Dir. Geol., 2005. Carte géologique du Maroc No461: Azrou - Échelle 1:50.000. Royaume du Maroc, Ministère l'Énergie des Mines du Développement Durable.

Domènech, M., Stockli, D.F., Teixell, A., 2018. Detrital zircon U–Pb provenance and palaeogeography of Triassic rift basins in the Marrakech High Atlas. Terra Nova 30, 310–318. https://doi.org/10.1111/ter.12340.

Eddif, A., Gasquet, D., Hoepffner, C., Levresse, G., 2007. Age of the Wirgane granodiorite intrusions (Western High-Atlas, Morocco): New U–Pb constraints. J. Afr. Earth Sci. 47, 227–231. https://doi.org/10.1016/j.jafrearsci.2007.02.003.

El Hadi, H., Simancas, J.F., Tahiri, A., Gonzalez-Lodeiro, F., Azor, A., Martinez-Poyatos, D., 2006. Comparative review of the Variscan granitoids of Morocco and Iberia: proposal of a broad zonation. Geodin. Acta 19, 103–116. https://doi.org/10.3166/ga.19.103-116.

El Hassani, A., Tahiri, A., Walliser, O.H., 2003. The Variscan crust between Gondwana and Baltica. CFS Courier Forschungsinstitut Senckenberg, pp. 81–87.

El Houicha, M., Pereira, M.F., Jouhari, A., Gama, C., Ennih, N., Fekkak, A., Ezzouhairi, H., El Attari, A., Silva, J.B., 2018. Recycling of the Proterozoic crystalline basement in the Coastal Block (Moroccan Meseta): new insights for understanding the geodynamic evolution of the northern peri-Gondwanan realm. Precambrian Res. 306, 129–154. https://doi.org/10.1016/j.precamres.2017.12.039.

Fedo, C.M., Sircombe, K.N., Rainbird, R.H., 2003. Detrital zircon analysis of the sedimentary record. Rev. Mineral. Geochem. 53, 277–303. https://doi.org/10.2113/0530277.

Fernández-Suárez, J., Corfu, F., Arenas, R., Marcos, A., Martínez Catalán, J., García, F., Abati, J., Fernández, F., 2002. U-Pb evidence for a polyorogenic evolution of the HP-HT units of the NW Iberian Massif. Contrib. Mineral. Petrol. 143, 236–253. https://doi.org/10.1007/s00410-001-0337-2.

Fernández-Suárez, J., Gutiérrez-Alonso, G., Pastor-Galán, D., Hofmann, M., Murphy, J.B., Linnemann, U., 2014. The Ediacaran–Early Cambrian detrital zircon record of NW Iberia: possible sources and paleogeographic constraints. Int. J. Earth Sci. 103, 1335–1357. https://doi.org/10.1007/s00531-013-0923-3.

Franke, W., Cocks, L.R.M., Torsvik, T.H., 2017. The Palaeozoic Variscan oceans revisited. Gondwana Res. 48, 257–284. https://doi.org/10.1016/j.gr.2017.03.005.

Ghienne, J.F., Benvenuti, A., El Houicha, M., Girard, F., Kali, E., Khoukhi, Y., Langbour, C., Magna, T., Míková, J., Moscariello, A., Schulmann, K., 2018. The impact of the end-Ordovician glaciation on sediment routing systems: a case study from the Meseta (northern Morocco). Gondwana Res. 63, 169–178. https://doi.org/10.1016/j.gr.2018.07.001.

Gutiérrez-Alonso, G., Fernández-Suárez, J., Pastor-Galán, D., Johnston, S.T., Linnemann, U., Hofmann, M., Shaw, J., Colmenero, J.R., Hernández, P., 2015. Significance of detrital zircons in Siluro-Devonian rocks from Iberia. J. Geol. Soc. Lond. 172, 309–322. https://doi.org/10.1144/jgs2014-118.

Hoepffner, C., 1977. Données nouvelles sur le Paléozoïques de la bordure occidentale du massif du Tazekka. 284. Comptes Rendus de l'Académie de Science de Paris, pp. 1635–1637.

Hoepffner, C., 1981. Le complexe volcano-sédimentaire d'âge carbonifère dans le massif du Tazekka, sa place dans l'évolution hercynienne de la Méséta marocaine orientale. Sci. Géol. Bull. Mém. 34, 97–106.

Hoepffner, C., 1987. La tectonique hercynienne dans l'Est du Maroc. Université Louis Pasteur, Strasbourg.

Hoepffner, C., 1989. L'évolution structurale hercynienne de la Méséta marocain orientale. Essai de mise au point. Notes et Mémoires du Service Géologique du Maroc.

Hoepffner, C., Houari, M.R., Bouabdelli, M., 2006. Tectonics of the North African Variscides (Morocco, western Algeria): an outline. Comptes Rendus - Géoscience 338, 25–40. https://doi.org/10.1016/j.crte.2005.11.003.

Hoepffner, C., Soulaimani, A., Piqué, A., 2005. The Moroccan Hercynides. J. Afr. Earth Sci. 43, 144–165. https://doi.org/10.1016/j.jafrearsci.2005.09.002.

Horon, O., 1952. Contribution à l'étude du bassin de Djerada. Notes et Mémoires du Protectorat de la République Française au Maroc 89. p. 180.

Houari, M.R., Hoepffner, C., 2003. Late Carboniferous dextral wrench-dominated transpression along the North African craton margin (Eastern High-Atlas, Morocco). J. Afr. Earth Sci. 37, 11–24. https://doi.org/10.1016/S0899-5362(03)00085-X.

Huvelin, P., 1970. Chevauchements et écaillages précoces hercyniens des terrains antéviséens dans le domaine atlasique (Maroc). 270. Comptes Rendus de l'Académie des Sciences de Paris, pp. 2760–2763.

Kharbouch, F., Juteau, T., Treuil, M., Joron, J.-L., Pique, A., Hoepffner, C., 1989. Le complexe volcano-sédimentaire hercynien de la Méséta marocaine nord-occidentale et orientale: étude pétrographique, géochimique et signification géodynamique. Notes et Mémoires du Service Géologique du Maroc.

Khoukhi, Y., Hamoumi, N., 2001. L'Ordovicien de la Meseta oriental (Maroc): stratigraphie génétique-contrôle géodynamique, climatique et eustatique. Afric. Geosci. Rev. 8, 289–302.

Lazreq, N., 1999. Biostratigraphie des conodontes du Givétien au Famennien du Maroc central: biofaciés et évènement Kellwasser. CFS Courier Forschungsinstitut Senckenberg 214.

Le Heron, D.P., 2007. Late Ordovician glacial record of the Anti-Atlas, Morocco. Sediment. Geol. 201, 93–110. https://doi.org/10.1016/j.sedgeo.2007.05.004.

Le Heron, D.P., Craig, J., Etienne, J.L., 2009. Ancient glaciations and hydrocarbon accumulations in North Africa and the Middle East. Earth Sci. Rev. 93, 47–76. https://doi.org/10.1016/j.earscirev.2009.02.001.

Letsch, D., El Houicha, M., von Quadt, A., Winkler, W., 2018. A missing link in the peri-Gondwanan terrane collage: the Precambrian basement of the Moroccan Meseta and its lower Paleozoic cover. Can. J. Earth Sci. 55, 1–19. https://doi.org/10.1139/cjes-2017-0086.

Linnemann, U., McNaughton, N.J., Romer, R.L., Gehmlich, M., Drost, K., Tonk, C., 2004. West African provenance for Saxo-Thuringia (Bohemian Massif): did Armorica ever leave pre-Pangean Gondwana? - U-Pb-SHRIMP zircon evidence and the Nd-isotopic record. Int. J. Earth Sci. 93, 683–705. https://doi.org/10.1007/s00531-004-0413-8.

Linnemann, U., Ouzegane, K., Drareni, A., Hofmann, M., Becker, S., Gärtner, A., Sagawe, A., 2011. Sands of West Gondwana: an archive of secular magmatism and plate interactions - a case study from the Cambro-Ordovician section of the Tassili Ouan Ahaggar (Algerian Sahara) using U-Pb-LA-ICP-MS detrital zircon ages. Lithos 123, 188–203. https://doi.org/10.1016/j.lithos.2011.01.010.

Linnemann, U., Pereira, M.F., Jeffries, T.E., Drost, K., Gerdes, A., 2008. The Cadomian Orogeny and the opening of the Rheic Ocean: the diacrony of geotectonic processes constrained by LA-ICP-MS U-Pb zircon dating (Ossa-Morena and Saxo-Thuringian Zones, Iberian and Bohemian Massifs). Tectonophysics 461, 21–43. https://doi.org/10.1016/j.tecto.2008.05.002.

Marhoumi, M.R., 1984. Étude palynologique des séries dinantiennes de la Méséta marocaine. Université Louis Pasteur, Strasbourg, Conséquences stratigraphiques et structurales.

Marhoumi, M.R., Doubinger, J., Rauscher, R., Hoepffner, C., 1989. Données nouvelles sur le Paléozoïque de la Méséta oriental marocaine. Apports de la palynologie. Notes et Mémoires du Service Géologique du Maroc.

Marhoumi, M.R., Hoepffner, C., Doubinger, J., Rauscher, R., 1983. Données nouvelles sur l'histoire hercynienne de la Meseta orientale au Maroc: l'âge dévonien des schistes de Debdou et du Mekkam. 297. Comptes Rendus de l'Académie des Sciences de Paris, pp. 69–72.

Marhoumi, M.R., Rauscher, R., 1984. Un plancton dévonien de la Meseta Orientale au Maroc. Rev. Palaeobot. Palynol. 43, 237–253. https://doi.org/10.1016/0034-6667(84)90035-6.

Marie, P., 1931. Rapport sur les observations faites pendant le mois de Février 1931 dans la région de Debdou Archives B.R.G.M., unpublished.

Marzoli, A., Davies, J.H.F.L., Youbi, N., Merle, R., Dal Corso, J., Dunkley, D.J., Fioretti, A.M., Bellieni, G., Medina, F., Wotzlaw, J.F., McHone, G., Font, E., Bensalah, M.K., 2017. Proterozoic to Mesozoic evolution of North-West Africa and Peri-Gondwana microplates: detrital zircon ages from Morocco and Canada. Lithos 278–281, 229–239. https://doi.org/10.1016/j.lithos.2017.01.016.

Matte, P., 2001. The Variscan collage and orogeny (480–290 Ma) and the tectonic definition of the Armorica microplate: a review. Terra Nova 13, 122–128. https://doi.org/10.1046/j.1365-3121.2001.00327.x.

Medioni, R., 1980. Mise au point stratigraphique sur les terrains carbonifères de la bordure septentrionale des Hauts-Plateaux marocains (massifs de Debdou, boutonnières de Lalla-Mimouna et du Mekam). Notes Serv. Géol. Maroc 285 (41), 25–37.

Michard, A., 1976. Éléments de géologie marocaine. Notes et Mémoires du Service Géologique du Maroc 252. p. 408.

Michard, A., Cailleux, Y., Hoepffner, C., 1989. L'orogène mésétien du Maroc: structure, déformation hercynienne et déplacement. Notes et Mémoires du Service Géologique du Maroc.

Michard, A., Ouanaimi, H., Hoepffner, C., Soulaimani, A., Baidder, L., 2010a. Comment on tectonic relationships of Southwest Iberia with the allochthons of Northwest Iberia and the Moroccan Variscides by J.F. Simancas et al. [C. R. Géoscience 341 (2009) 103–113]. Compt. Rend. Géosci. 342, 170–174. https://doi.org/10.1016/j.crte.2010.01.008.

Michard, A., Saddiqi, O., Chalouan, A., Frizon de Lamotte, D., 2008. Continental evolution: the geology of Morocco. Springer https://doi.org/10.1007/978-3-540-75761-0.

Michard, A., Soulaimani, A., Hoepffner, C., Ouanaimi, H., Baidder, L., Rjimati, E.C., Saddiqi, O., 2010b. The south-western branch of the Variscan belt: evidence from Morocco. Tectonophysics 492, 1–24. https://doi.org/10.1016/j.tecto.2010.05.021.

Montero, P., Talavera, C., Bea, F., Lodeiro, F.G., Whitehouse, M.J., 2009. Zircon geochronology of the Ollo de Sapo Formation and the age of the Cambro-Ordovician rifting in Iberia. J. Geol. 117, 174–191. https://doi.org/10.1086/595017.

Murphy, J.B., Fernández-Suárez, J., Keppie, J.D., Jeffries, T.E., 2004. Contiguous rather than discrete Paleozoic histories for the Avalon and Meguma terranes based on detrital zircon data. Geology 32, 585–588. https://doi.org/10.1130/G20351.1.

Naidoo, T., Zimmermann, U., Vervoort, J., Tait, J., 2018. Evidence of early Archean crust in northwest Gondwana, from U–Pb and Hf isotope analysis of detrital zircon, in Ediacaran supracrustal rocks of northern Spain. Int. J. Earth Sci. 107, 409–429. https://doi.org/10.1007/s00531-017-1500-y.

Nance, R.D., Gutiérrez-Alonso, G., Keppie, J.D., Linnemann, U., Murphy, J.B., Quesada, C., Strachan, R.A., Woodcock, N.H., 2010. Evolution of the Rheic Ocean. Gondwana Res. 17, 194–222. https://doi.org/10.1016/j.gr.2009.08.001.

Nance, R.D., Gutiérrez-Alonso, G., Keppie, J.D., Linnemann, U., Murphy, J.B., Quesada, C., Strachan, R.A., Woodcock, N.H., 2012. A brief history of the Rheic Ocean. Geosci. Front. 3, 125–135. https://doi.org/10.1016/j.gsf.2011.11.008.

Nance, R.D., Murphy, J.B., Strachan, R.A., Keppie, J.D., Gutiérrez-Alonso, G., Fernández-Suárez, J., Quesada, C., Linnemann, U., D'lemos, R., Pisarevsky, S.A., 2008. Neoproterozoic-early Palaeozoic tectonostratigraphy and palaeogeography of the peri-Gondwanan terranes: Amazonian v. West African connections. Geol. Soc. Lond. 297, 345–383. https://doi.org/10.1144/SO297.17 Special Publication.

Ouabid, M., Ouali, H., Garrido, C.J., Acosta-Vigil, A., Román-Alpiste, M.J., Dautria, J.M., Marchesi, C., Hidas, K., 2017. Neoproterozoic granitoids in the basement of the Moroccan Central Meseta: correlation with the Anti-Atlas at the NW paleo-margin of Gondwana. Precambrian Res. 299, 34–57. https://doi.org/10.1016/j.precamres.2017.07.007.

Pastor-Galán, D., Gutiérrez-Alonso, G., Murphy, J.B., Fernández-Suárez, J., Hofmann, M., Linnemann, U., 2013. Provenance analysis of the Paleozoic sequences of the northern Gondwana margin in NW Iberia: passive margin to Variscan collision and orocline development. Gondwana Res. 23, 1089–1103. https://doi.org/10.1016/j.gr.2012.06.015.

Pereira, M.F., Chichorro, M., Johnston, S.T., Gutiérrez-Alonso, G., Silva, J.B., Linnemann, U., Hofmann, M., Drost, K., 2012. The missing Rheic Ocean magmatic arcs: provenance analysis of Late Paleozoic sedimentary clastic rocks of SW Iberia. Gondwana Res. 22, 882–891. https://doi.org/10.1016/j.gr.2012.03.010.

Pereira, M.F., El Houicha, M., Chichorro, M., Armstrong, R., Jouhari, A., El Attari, A., Ennih, N., Silva, J.B., 2015. Evidence of a Paleoproterozoic basement in the Moroccan Variscan belt (Rehamna Massif, Western Meseta). Precambrian Res. 268, 61–73. https://doi.org/10.1016/j.precamres.2015.07.010.

Pereira, M.F., Gutiérrez-Alonso, G., Murphy, J.B., Drost, K., Gama, C., Silva, J.B., 2017. Birth and demise of the Rheic Ocean magmatic arc(s): combined U-Pb and Hf isotope analyses in detrital zircon from SW Iberia siliciclastic strata. Lithos 278–281, 383–399. https://doi.org/10.1016/j.lithos.2017.02.009.

Pérez-Cáceres, I., Martínez Poyatos, D., Simancas, J.F., Azor, A., 2017. Testing the Avalonian affinity of the South Portuguese Zone and the Neoproterozoic evolution of SW Iberia through detrital zircon populations. Gondwana Res. 42, 177–192. https://doi.org/10.1016/j.gr.2016.10.010.

Pérez-Estaún, A., Bastida, F., Martínez Catalán, J.R., Gutiérrez-Marco, J.C., Marcos, A., Pulgar, J.A., 1990. The West-Asturian Leonese zone. Stratigraphy. In: Dallmeyer, R.D., Martínez García, E. (Eds.), Pre-Mesozoic Geology of Iberia. Springer-Verlag, Berlin, pp. 92–102.

Piqué, A., 2001. Geology of Northwest Africa. Borntraeger, Berlin.

Piqué, A., Michard, A., 1981. Les zones structurales du Maroc hercynien. Sci. Géol. Bull. Mém. 34, 135–146.

Piqué, A., Michard, A., 1989. Moroccan Hercynides: a synopsis. The Paleozoic sedimentary and tectonic evolution at the northern margin of West Africa. Am. J. Sci. 289, 286–330.

Pouclet, A., El Hadi, H., Álvaro, J.J., Bardintzeff, J.-M., Benharref, M., Fekkak, A., 2018. Review of the Cambrian volcanic activity in Morocco: geochemical fingerprints and geotectonic implications for the rifting of West Gondwana. Int. J. Earth Sci. 107, 2101–2123. https://doi.org/10.1007/s00531-018-1590-1.

Pratt, J.R., Barbeau, D.L., Garver, J.I., Emran, A., Izykowski, T.M., 2015. Detrital zircon geochronology of Mesozoic sediments in the Rif and Middle Atlas belts of Morocco: provenance constraints and refinement of the West African signature. J. Geol. 123, 177–200. https://doi.org/10.1086/681218.

Rauscher, R., Marhoumi, M.R., Vanguestaine, M., Hoepffner, C., 1982. Datation palynologique des schistes du Tazekka au Maroc. Hypothèse structurale sur le socle hercynien de la Meseta orientale. 294. Comptes Rendus de l'Académie de Science de Paris, pp. 1203–1206.

Said, I., Rodríguez, S., Berkhli, M., Cózar, P., Gómez-Herguedas, A., 2010. Environmental parameters of a coral assemblage from the Akerchi Formation (Carboniferous), Adarouch area, central Morocco. J. Iber. Geol. 36 (1), 7–19.

Shaw, J., Gutiérrez-Alonso, G., Johnston, S.T., Pastor Galán, D., 2014. Provenance variability along the Early Ordovician north Gondwana margin: paleogeographic and tectonic implications of U-Pb detrital zircon ages from the Armorican Quartzite of the Iberian Variscan belt. Bull. Geol. Soc. Am. 126, 702–719. https://doi.org/10.1130/B30935.1.

Simancas, J.F., Azor, A., Martínez-Poyatos, D., Tahiri, A., El Hadi, H., González-Lodeiro, F., Pérez-Estaún, A., Carbonell, R., 2009. Tectonic relationships of Southwest Iberia with the allochthons of Northwest Iberia and the Moroccan Variscides. Comp. Rend. – Géosci. 341, 103–113. https://doi.org/10.1016/j.crte.2008.11.003.

Simancas, J.F., Azor, A., Martínez-Poyatos, D., Tahiri, A., El Hadi, H., González-Lodeiro, F., Pérez-Estaún, A., Carbonell, R., 2010. Reply to the comment by Michard et al. on "Tectonic relationships of Southwest Iberia with the allochthons of Northwest Iberia and the Moroccan Variscides". Compt. Rendus Géosci. 342, 175–177. https://doi.org/10.1016/j.crte.2010.01.007.

Simancas, J.F., Tahiri, A., Azor, A., Lodeiro, F.G., Martínez Poyatos, D.J., El Hadi, H., 2005. The tectonic frame of the Variscan-Alleghanian orogen in southern Europe and northern Africa. Tectonophysics 398, 181–198. https://doi.org/10.1016/j.tecto.2005.02.006.

Slagstad, T., Roberts, N.M.W., Kulakov, E., 2017. Linking orogenesis across a supercontinent; the Grenvillian and Sveconorwegian margins on Rodinia. Gondwana Res. 44, 109–115. https://doi.org/10.1016/j.gr.2016.12.007.

Tahiri, A., Montero, P., El Hadi, H., Martínez Poyatos, D., Azor, A., Bea, F., Simancas, J.F., González Lodeiro, F., 2010. Geochronological data on the Rabat-Tiflet granitoids: their bearing on the tectonics of the Moroccan Variscides. J. Afr. Earth Sci. 57, 1–13. https://doi.org/10.1016/j.jafrearsci.2009.07.005.

Tahiri, A., El Hadi, H., Pocelet, A., Martínez Poyatos, D.J., Azor, A., Lodeiro, F., Simancas, F., 2017. Ediacaran to Cambrian U-Pb ages of granite pebbles in the Lower Devonian conglomerate of Imouzzer Kandar (northwestern Middle Atlas, Morocco). In: The First West African Craton and Margins International Workshop "WACMAt" (Abstract). Morocco, Dakhla.

Talavera, C., Montero, P., Martínez Poyatos, D., Williams, I.S., 2012. Ediacaran to Lower Ordovician age for rocks ascribed to the Schist–Graywacke Complex (Iberian Massif, Spain): evidence from detrital zircon SHRIMP U–Pb geochronology. Gondwana Res. 22, 928–942. https://doi.org/10.1016/j.gr.2012.03.008.

Valin, F., 1979. Stratigraphie du paléozoïque dans les monts d'Oujda (Maroc oriental). Mines, Géologie et Énergie 46. pp. 79–81.

Vermeesch, P., 2004. How many grains are needed for a provenance study? Earth Planet. Sci. Lett. 224, 441–451. https://doi.org/10.1016/j.epsl.2004.05.037.

Vermeesch, P., 2012. On the visualization of detrital age distributions. Chem. Geol. 312–313, 190–194. https://doi.org/10.1016/j.chemgeo.2012.04.021.

Vermeesch, P., 2018. IsoplotR: a free and open toolbox for geochronology. Geosci. Front. 9, 1479–1493. https://doi.org/10.1016/j.gsf.2018.04.001.

Vidal, J.C., Hoepffner, C., 1979. Carte géologique du Rif No282: Tahala - Échelle 1/50.000. Royaume du Maroc, Ministère l'Énergie des Mines du Développement Durable.

Villeneuve, M., 2008. Review of the orogenic belts on the western side of the West African Craton: the Bassarides, Rokelides and Mauritanides. Geol. Soc. Lond. Spec. Publ. 297, 169–201. https://doi.org/10.1144/SP297.8.

Walliser, O.H., El Hassani, A., Tahiri, A., 1995. Sur le Dévonien de la Meseta marocaine occidentale. Comparaisons avec le Dévonien allemand et évènements globaux. CFS Cour. Forschung. Senckenberg 188, 21–30.

Walliser, O.H., El Hassani, A., Tahiri, A., 2000. Mrirt: a key area for the Variscan Meseta of Morocco. Notes et Mémoires du Service Géologique du Maroc. 399 pp. 93–108.

Wollen, I.D., 1974. Structure, stratigraphy and environmental analysis of the Lower Carboniferous rocks near Azrou. University of South Carolina.